A GEOMETRIC LITTLEWOOD-RICHARDSON RULE

RAVI VAKIL

CONTENTS

The real goal of this note is to spell out the details of the proof. After consulting with experts (esp. Allen, Anders, and Frank) to correct my notation, add references to the literature, and trim arguments that are well-known, I intend to write a paper based on this. (Hence please don't pass this on to anyone else — it isn't suitable for public consumption.) Sections 2–5 may resemble their final form, but Section 6 is a looser collection of thoughts and the bibliography is embryonic. I intend to give copies to Anders Buch, Linda Chen, Bill Fulton, Allen Knutson, Greg Landweber, Leonardo Mihalcea, Frank Sottile, and possibly Bob MacPherson and Zvezda Stankova.

Notational asides: (i) The "quilt varieties" of Section 4 are straightforward objects, and undoubtedly have been defined before. I wouldn't mind referring to earlier work and excising all or most of Section 4. I'd called them "Bott-Samelson varieties" (and the corresponding posets "Bott-Samuelson posets") until last week, when a preprint on math.AG made me realize that the term "Bott-Samelson varieties" was already taken! I flailed about for a new terminology (skeleton varieties? poset-filtered varieties?), and have temporarily settled on quilt varieties, but suggestions from the poetically-minded would be appreciated. (ii) Anders suggested using the more attractive $F_\bullet$ *rather than* $F_.$*. However, I'm using* $\bullet$ *to mean something important (a configuration of black checkers), and I don't want readers to be confused that the subscript in* $F_\bullet$ *means something as it does in* $X_\bullet$*, so I'm leaning toward staying with* $F_.$*.*

Date: Sunday, May 5, 2002, 11 am.
Partially supported by NSF Grant DMS–0098769 and an AMS Centennial Fellowship.

1. Introduction

The goal of this note is to describe an explicit geometric Littlewood-Richardson rule, by way of deforming the intersection of two Schubert cells (with respect to transverse flags $F_\cdot^{\text{fixed}}$ and $F_\cdot^{\text{moving}}$) so that they break into Schubert cells. This should be seen as a generalization of Pieri's rule to arbitrary Schubert classes, by way of explicit homotopies.

The strategy is as follows. We degenerate $F_\cdot^{\text{moving}}$ through a series of codimension one degenerations (in $Fl(n)$) in a particular way (the "degeneration sequence") so that the cycle in $G(k,n)$ successively breaks into varieties we can easily understand ("two-flag Schubert varieties"). At each stage, the cycle breaks into one or two pieces, and each piece appears with multiplicity one (a key fact for applications). At the end the two flags $F_\cdot^{\text{fixed}}$ and $F_\cdot^{\text{moving}}$ coincide, and the limit is a union of Schubert varieties with respect to this flag. I believe this degeneration approach is the same strategy originally used to prove both Pieri's formula and Monk's rule, but I will check to make sure. An explicit example is shown in Figure 6. (*Caution:* the theorem is stated in terms of the affine description of the Grassmannian, but all geometric descriptions are in terms of the projective description. Hence Figure 6 shows a calculation in $G(2,4)$ using lines in $\mathbb{P}^3$.)

The degenerations can be described combinatorially, in terms of black and white checkers on an $n \times n$ checkerboard. Thus Littlewood-Richardson coefficients count "checker games". The input is the data of two Schubert cells, in the form of two k-subsets of $\{1,\dots,n\}$; each move corresponds to moving black checkers (encoding the position of $F_\cdot^{\text{moving}}$) in a certain way (the "degeneration sequence"), and determining then how the white checkers (encoding the position of the k-plane) move. The output is interpreted as set of k-subsets. Similarly, Schubert problems (i.e. intersecting many Schubert classes) count "checker tournaments". The checker rule is easy to use in practice, but somewhat awkward to describe. However, (i) its geometric meaning is clear at all steps, and (ii) there is a straightforward bijection [KV] between checker games and Knutson and Tao's beautiful puzzles, [KTW, KT]. For many geometric applications, the details of the combinatorial rule are unnecessary. R. Moriarty has written a program implementing this rule (as part of an undergraduate research program).

As applications, (i) it gives a Littlewood-Richardson rule with explicit geometric meaning (and in particular a geometric interpretation of puzzles), (ii) all Schubert problems on all Grassmannians can have all real solutions (the "reality problem" for Grassmannians), generalizing work of F. Sottile, (iii) it gives the first means of solving all Schubert problems numerically, generalizing work of Huber, Sottile, and Sturmfels, and (iv) it gives to an approach to the Littlewood-Richardson problem for the flag variety, leading to an explicit conjecture which is true up to dimension 5 (implying, for example, that all Schubert problems in these cases can have real solutions). Also, the geometric description of the rule gives a promising approach to other variants (all of which are currently open): (v) a conjectured K-theory checker rule of Buch which implies a conjectured puzzle rule of Tao's, (vi) Littlewood-Richardson rules for other groups, e.g. the Lagrangian Grassmannian, (vii) two-step flag varieties, possibly via a puzzle conjecture of Knutson's, which would give Littlewood-Richardson coefficients in quantum cohomology, and more.

1.1. Overview of paper. Section 2 is a description of the rule in combinatorial terms; it contains no geometry.

Section 3 describes the geometry related to "two-flag Schubert cells" in the Grassmannian in the language of checkers. Black checkers correspond to the relative position of the two flags; white checkers correspond to the k-plane. The main theorem (Theorem 3.10) is stated here. Readers of a geometric bent may prefer to read some of Section 3 before Section 2.

The proof makes repeated use of smooth "quilt varieties" $Q(\mathcal{P})$ corresponding to a "planar poset" $\mathcal{P}$. They are simple objects, and some basic properties are described in Section 4. Of particular importance is the quilt variety $Q(\mathcal{P}_\square)$ parametrizing two hyperplanes and a codimension two plane contained in both. Each step in the degeneration is related to $Q(\mathcal{P}_\square)$ via the key construction of Section 4.5.

The proof of the Geometric Littlewood-Richardson rule is given in Section 5; the strategy is outlined in Section 5.1.

Applications are discussed in Section 6. Some are proved in detail, while others are merely sketched.

1.2. *Summary of notation.* If $X \subset Y$, let $\mathrm{Cl}_Y X$ denote the closure in Y of X. Fix a base field K (of any characteristic, not necessarily algebraically closed), and non-negative integers $k \leq n$. We work in $G(k,n)$, the Grassmannian of dimension k subspaces of (a fixed) K^n. [1]

We follow the notation of [F]. For example, let Ω_w denote the Schubert class in $H^*(G(k,n))$ (resp. $H^*(Fl(n))$), where w is a partition (resp. a permutation). Let $\Omega_w(F.)$ (resp. $\Omega^\circ_w(F.)$) be the closed (resp. open) Schubert variety with respect to the flag $F.$. In $Fl(n)$,

$$\Omega_w(F.) = \{[V.] \in Fl(n) : \dim(V_p \cap F_q) \geq \#\{i \leq p : w(i) > n-q\} \text{ for all } p, q\}.$$

The Schur polynomials are denoted $s.$.

When I turn this into a paper, I intend to have a list here summarizing important notation for the reader's benefit. For now, I have used footnotes, which are more convenient but uglier.

1.3. Acknowledgments (in no particular order; will be trimmed in the paper). The author is grateful to A. Buch and A. Knutson for patiently explaining the combinatorial, geometric, and representation-theoretic ideas behind this problem. Any remaining misunderstandings are purely due to the author. The author also thanks L. Chen, W. Fulton, R. Moriarty, and F. Sottile; MSRI for hospitality when this was written up; D. Eisenbud for his comment of Section 6.9; and B. Sturmfels for pointing out that the Geometric Littlewood-Richardson rule should give a means of numerically solving Schubert problems.

[1] Cl, K

2. The Geometric Littlewood-Richardson rule: Combinatorial description

Littlewood-Richardson coefficients $c^{\gamma}_{\alpha\beta}$ will be counted in their guise of structure constants of the cohomology (or Chow) ring of the Grassmannian $G(k,n)$, which in turn will be interpreted in terms of *checker games*, involving n black and k white checkers on an $n \times n$ board. The rows and columns of the board are numbered as in Figure 1; (r,c) will denote the square in row r and column c. A set of checkers on the board will be called a *configuration* of checkers.[2]

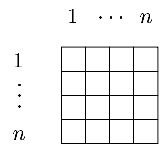

FIGURE 1.

2.1. Black checkers. The moves of the black checkers are prescribed in advance; the Littlewood-Richardson coefficients are counted by the possible accompanying moves of the white checkers.

No two checkers of the same color are in the same row or column. Hence the positions of the black checkers correspond to permutations by the following bijection: if the blacker in column c is in row r, then the permutation sends $n-c$ to r. For example, see Figure 2.

The initial position of the black checkers corresponds to the identity permutation in S_n, and the final position corresponds to the longest word w_0. The intermediate positions in the checker game correspond to partial factorizations from the right of w_0:

$$w_0 = e_{n-1}\cdots e_2 e_1 \quad \cdots \quad e_{n-1}e_{n-2}e_{n-3} \quad e_{n-1}e_{n-2} \quad e_{n-1}.$$

For example, in Figure 2 shows the six moves of the black checkers for $n=4$, along with the corresponding permutations. (The geometric interpretation will be explained in Section 3.3.) In essence this is a bubble-sort. Call this the *degeneration sequence* in the Bruhat order. Figure 3 shows a typical checker configuration in the degeneration sequence. Each move will involve moving one checker one row down (call this the *descending checker*), and another checker (call this the *rising checker*)[3] one row up, as shown in the figure.

We will use the notation $\bullet$ to represent a configuration of black checkers. Denote the initial configuration by $\bullet_{\text{init}}$, and the final configuration by $\bullet_{\text{final}}$. If $\bullet$ is one of the configurations in the degeneration sequence, and $\bullet \neq \bullet_{\text{final}}$, then $\bullet_{\text{next}}$ will denote the next configuration in the degeneration sequence.[4]

[2] configuration of checkers

[3] degeneration sequence; descending and rising checker; should this be ascending, or descending should be falling?

[4] $\bullet$, $\bullet_{\text{init}}$, $\bullet_{\text{final}}$, $\bullet_{\text{next}}$

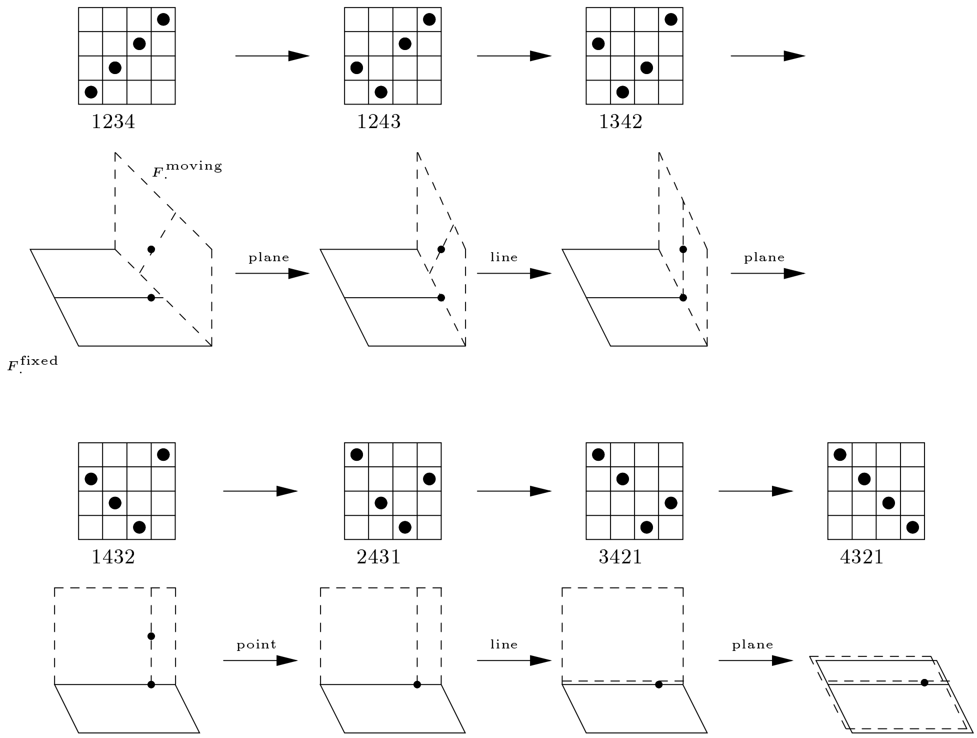

FIGURE 2. The *degeneration sequence* for $n = 4$, in terms of checkers and permutations, with the geometric interpretation of Section 3

2.2. White checkers. At each stage of the game, each white checker has the following property: there is a black checker in the same square or in a square above it, and there is a black checker in the same square or in a square to the left of it. A white checker satisfying this property is said to be *happy*. (In particular, a white checker is happy if it is in the same square as a black checker.) A configuration of white checkers will often be denoted $\circ$, and a configuration of white and black checkers will often be denoted $\circ\bullet$.[5]

The initial position of the white checkers depends on two subsets $A = \{a_1, \ldots, a_k\}$ and $B = \{b_1, \ldots, b_k\}$ of $\{1, \ldots, n\}$, where $a_1 < \cdots < a_k$ and $b_1 < \cdots < b_k$. The k white checkers are in the squares (a_1, b_k), (a_2, b_{k-1}), …, (a_k, b_1). We denote this configuration by $\circ_{A,B}$.[6] If (and only if) any of these white checkers are not happy (i.e. if $a_i + b_{k+1-i} \leq n$ for some i), then there are no checker games corresponding to (A, B). (This will mean that all corresponding Littlewood-Richardson coefficients are 0. Geometrically, this means that the two Schubert cells do not intersect.) This happens, for example, if $n = 2$ and $A = B = \{1\}$.

[5] happy, $\circ$, $\circ\bullet$

[6] $\circ_{A,B}$

<table>
<tr><td colspan="2" rowspan="2"></td><td colspan="3">White checker in critical row?</td></tr>
<tr><td>yes, in descending checker's square</td><td>yes, elsewhere</td><td>no</td></tr>
<tr><td rowspan="3">Top white checker in critical diagonal?</td><td>yes, in rising checker's square</td><td>swap</td><td>swap</td><td>stay</td></tr>
<tr><td>yes, elsewhere</td><td>swap</td><td>swap if no blocker or stay</td><td>stay</td></tr>
<tr><td>no</td><td>stay</td><td>stay</td><td>stay</td></tr>
</table>

TABLE 1. Phase 1 of the white checker moves

For each move of the black checkers, there will be one or two possible moves of the white checkers, which we describe next. Define the *critical row* and the *critical diagonal* as in Figure 3.[7] The movement of the white checkers takes place in two phases.

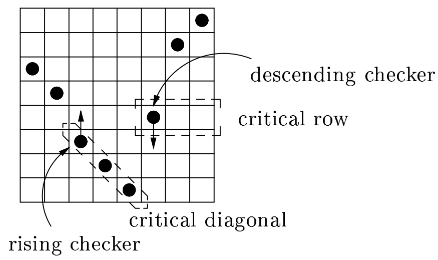

FIGURE 3. The critical row and the critical diagonal

Phase 1[8] depends on the answers to the two questions: Where (if anywhere) is the white checker in the critical row? Where (if anywhere) is the highest white checker in the critical diagonal? (There may be several white checkers in the critical diagonal.)

Based on the answer to these questions, the pair of white checkers either swap[9] rows (i.e. if the white checkers start at (r_1, c_1) and (r_2, c_2), then they will end at (r_2, c_1) and (r_1, c_2)), or they stay where they are, according to Table 1. The central entry of the table is the only time when there is a possibility for choice: the pair of white checkers can stay, or *if there are no white checkers in the rectangle between them* they can swap. Call white checkers in this rectangle *blockers*.[10] See Figure 4 for an example of a blocker.

Phase 2[11] is a "clean-up phase": if any white checkers are not happy, then move them by sliding them either left or up so that they become happy. This is always possible.

[7] critical row, critical diagonal
[8] Phase 1
[9] swap
[10] blocker
[11] Phase 2

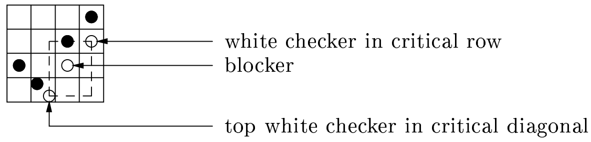

FIGURE 4. Example of a blocker

If $\circ\bullet$ corresponds to the configuration of black and white checkers before the move, we denote the one or two possible configurations after the move by $\circ_{\text{stay}}\bullet_{\text{next}}$ and/or $\circ_{\text{swap}}\bullet_{\text{next}}$.[12] Examples of the ten cases are given in Figure 5.

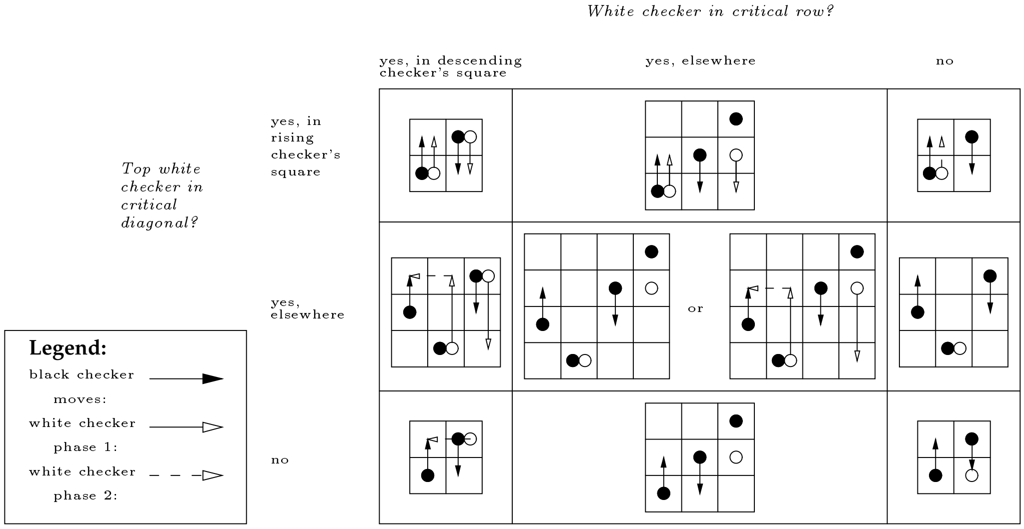

FIGURE 5. Examples of the nine cases

At the end of the checker game, the black checkers are in position $\bullet_{\text{final}}$, and as the white checkers are happy, they must lie on a subset of the black checkers. The corresponding output is again a subset S of $\{1, \ldots, n\}$ of order k. Denote this final configuration of white checkers by $\circ_S$.[13]

Hence to any two subsets A, B of $\{1, \ldots, n\}$ of order k, we can associate a formal sum of subsets of order k, corresponding to checker games. Figure 6 illustrates the two checker games starting with $A = B = \{2, 4\}$ for $k = 2$, $n = 4$. The output consists of the two subsets $\{1, 4\}$ and $\{2, 3\}$. Figure 7 illustrates all checker games starting with $A = B = \{2, 4, 6\}$ for $k = 3$, $n = 6$. The output is $\{2, 3, 4\} + 2\{1, 3, 5\} + \{1, 2, 6\}$.

2.3. Littlewood-Richardson coefficients in terms of checker games.

[12] $\circ_{\text{stay}}$, $\circ_{\text{swap}}$

[13] $\circ_S$

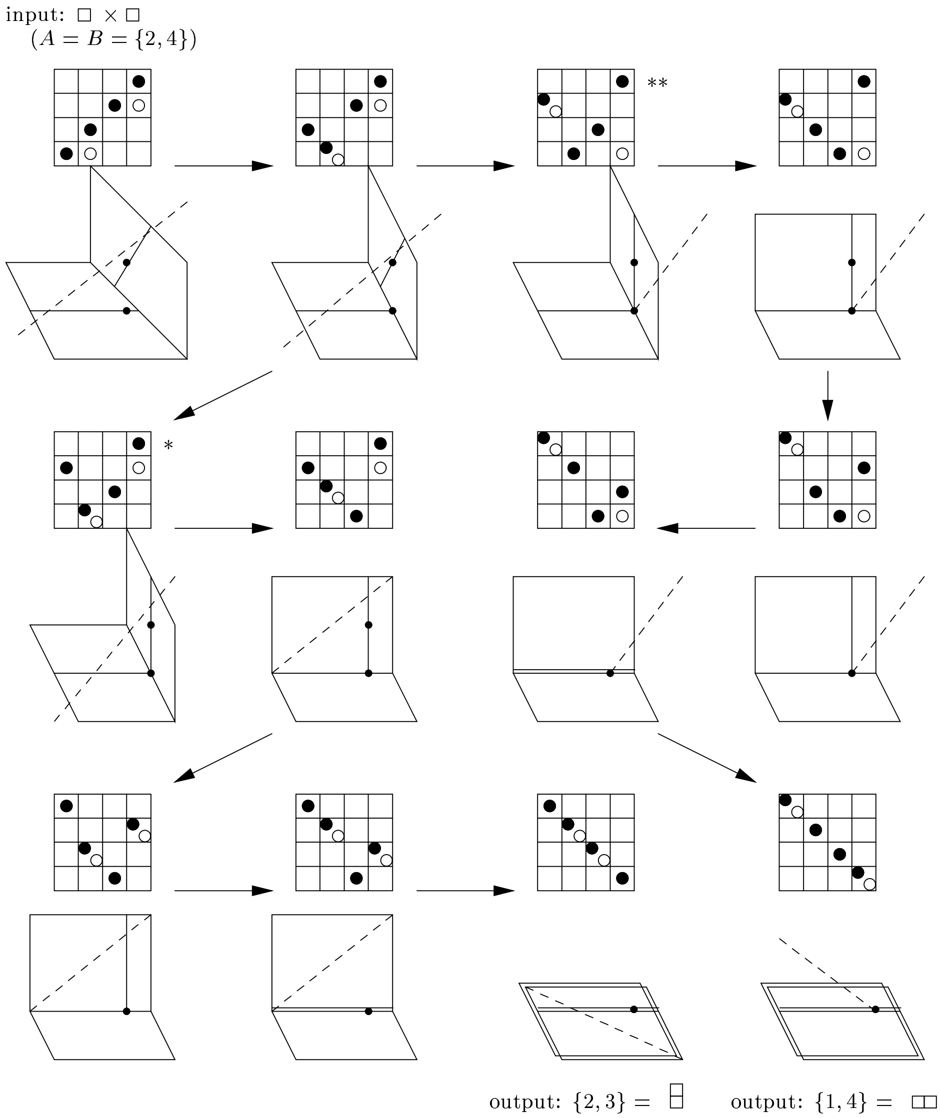

FIGURE 6. Two checker games with the same starting position, and the geometric interpretation of Section 3 (compare to Figure 2; checker configurations * and ** are discussed in Section 3.12)

Littlewood-Richardson rules give combinatorial descriptions of Littlewood-Richardson coefficients $c^{\gamma}_{\alpha\beta}$, defined by

$$s_\alpha s_\beta = \sum_\gamma c^{\gamma}_{\alpha\beta} s_\gamma$$

where α and β are partitions, and $s.$ are Schur functions. The checker games will compute compute the sum on the right modulo the ideal (in the ring of symmetric functions) defining the cohomology ring of the Grassmannian $G(k, n)$.

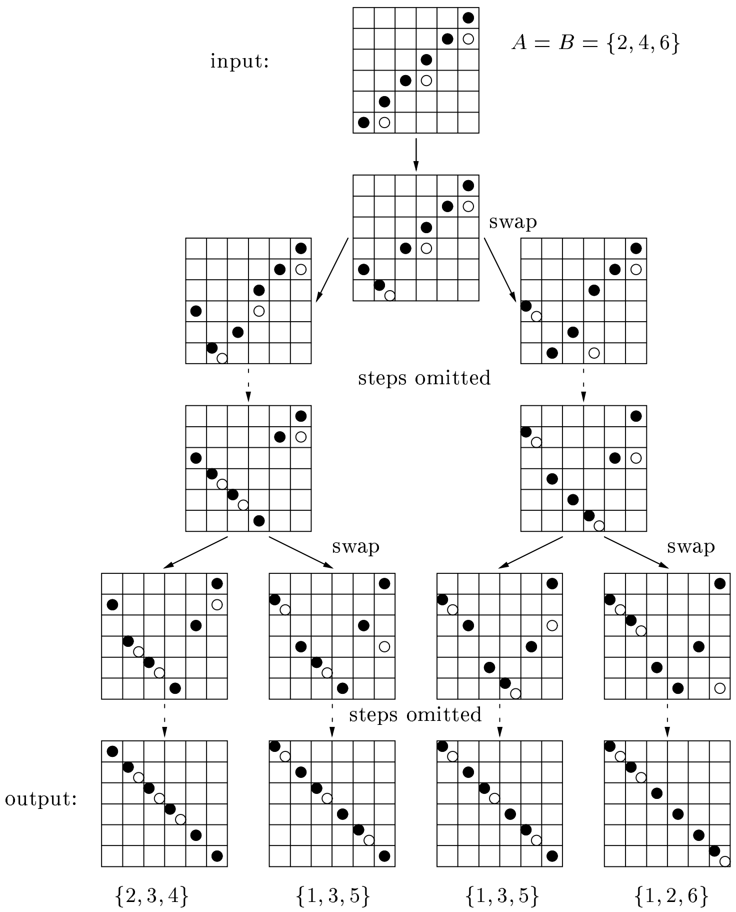

FIGURE 7. Computing $c_{(2,1),(2,1)}^{(3,2,1)} = 2$ using $k = 3$, $n = 6$; some intermediate steps are omitted

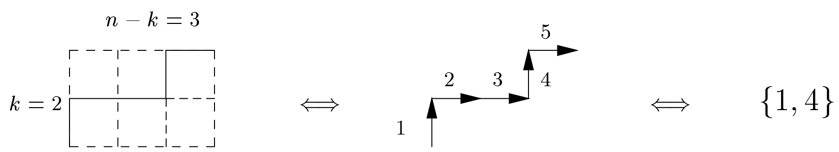

FIGURE 8. The bijection between $Rec_{k,n-k}$ and size k subsets of $\{1,\ldots,n\}$

More precisely, let $Rec_{k,n-k}$[14] be the set of subdiagrams of the rectangle with k rows and $n-k$ columns. Throughout this article, we identify $Rec_{k,n-k}$ with subsets of $\{1,\ldots,n\}$ of order k using the well-known bijection (see Figure 8). Fix α and β.

2.4. *Theorem (Geometric Littlewood-Richardson rule, first version).* —

[14] $Rec_{k,n-k}$

(a)

$$\sum_{\text{games } G} s_{\mathit{output}(G)} = \sum_{\gamma \in Rec_{k,n-k}} c^{\gamma}_{\alpha\beta} s_{\gamma}$$

where the left sum is over all checker games with input α and β, and output(G) is the output of checker game G.

(b) *Hence if $\gamma \in Rec_{k,n-k}$, then the integer $c^{\gamma}_{\alpha\beta}$ is the number of checker games starting with configuration $\circ_{\alpha,\beta}\bullet_{\mathrm{init}}$ and ending with configuration $\circ_{\gamma}\bullet_{\mathrm{final}}$.*

For example, Figure 6 computes $s^2_{(1)} = s_{(2)} + s_{(1,1)}$. Figure 7 computes $c^{(3,2,1)}_{(2,1),(2,1)} = 2$ using $k = 3$, $n = 6$.

Theorem 2.4 follows immediately from Theorem 3.9 (Geometric Littlewood-Richardson rule, second version).

2.5. *Remarks.* Like Pieri's formula and Monk's formula, this rule most naturally gives all terms in an intersection all at once (part (a)), but the individual coefficients can be easily extracted (part (b)).

A derivation of Pieri's formula from the Geometric Littlewood-Richardson rule is left as an exercise to the reader. Note that Pieri's original proof was also by degeneration methods.

Certain fundamental properties of Littlewood-Richardson coefficients are not clear from the Geometric Littlewood-Richardson rule, including:

(1) $c^{\gamma}_{\alpha\beta} = c^{\gamma}_{\beta\alpha}$.
(2) The rule is independent of the choice of n and k (i.e. the computation of $c^{\gamma}_{\alpha\beta}$ is independent of any n and k such that $\gamma \in Rec_{k,n-k}$).

The "triality" $c^{\gamma}_{\alpha\beta} = c^{\alpha^\vee}_{\beta\gamma^\vee}$ can be deduced most easily by way of the bijection to puzzles [KV].

We will need the following combinatorial observation.

2.6. *Lemma. — Suppose at some point in the algorithm, the descending checker is in column c. Suppose the white checkers are at $(r_1, c_1), \dots, (r_k, c_k)$ with $c_1 < \cdots < c_k$. Then $(r_1, \dots, r_k)$ is increasing for $c_i \leq c$ and decreasing for $c_i \geq c$.*

This follows from a straightforward induction showing that this property is preserved by each move. We say that configuration $\circ\bullet$ with this property is *mid-sort*.[15] For example, the white checkers of Figures 7 and 16 are mid-sort.

[15] mid-sort

3. Describing the geometry of the Grassmannian and flag variety with checkers

In this section, we interpret checker configurations geometrically, and state the main technical result of the paper, Theorem 3.10 (the Geometric Littlewood-Richardson rule, third version). Black checkers will correspond to the relative position of the two flags $F_\cdot^{\text{moving}}$ and $F_\cdot^{\text{fixed}}$, and white checkers will correspond to the position of the k-plane relative to the flags.

3.1. The relative position of two flags, given by black checkers; the variety $X_\bullet$. Given two flags $F_\cdot^{\text{moving}}$ and $F_\cdot^{\text{fixed}}$,[16] construct an $n \times n$ "rank" table of the numbers $\dim F_i^{\text{moving}} \cap F_j^{\text{fixed}}$. Up to the action of $GL(n)$, the two flags are specified by this table.

0	0	0	1
0	1	1	2
0	1	2	3
1	2	3	4

$\Longleftrightarrow$

			●
	●		
		●	
●			

FIGURE 9. The relative position of two flags, given by numbers on an $n \times n$ board, and by a configuration of black checkers

This data is equivalent to the data of n black checkers on the checkerboard such that no two are in the same row or column. The bijection is given as follows. We say a square (i_1, j_1) *dominates*[17] another square (i_2, j_2) if $i_1 \geq i_2$ and $j_1 \geq j_2$. Given the black checkers, $\dim F_i^{\text{moving}} \cap F_j^{\text{fixed}}$ is given by the number of black checkers dominated by square (i, j). An example of the bijection is given in Figure 9.

Note that each square in the table corresponds to a vector space, whose dimension is the number of black checkers dominated by that square. The vector space is the span of the vector spaces corresponding to the black checkers it dominates.

Let $X_\bullet$ be the (locally closed) subvariety of $Fl(n) \times Fl(n)$ corresponding to flags $(F_\cdot^{\text{moving}}, F_\cdot^{\text{fixed}})$ in relative position given by black checker configuration $\bullet$.[18] The variety $X_\bullet$ is smooth, and its codimension in $Fl(n) \times Fl(n)$ is the number of pairs of distinct black checkers a and b such that a dominates b. (This is a straightforward exercise; it also follows quickly from Section 4.)

3.2. *Side remark: Schubert cells of the flag variety.* For a fixed $F_\cdot^{\text{fixed}}$ and fixed configuration $\bullet$ of black checkers, the set of $F_\cdot^{\text{moving}}$ in $Fl(n)$ such that the relative position of $F_\cdot^{\text{moving}}$ and

[16] $F_\cdot^{\text{moving}}$, $F_\cdot^{\text{fixed}}$
[17] dominate
[18] $X_\bullet$

$F_.^{\text{fixed}}$ is given by $\bullet$ is an open Schubert cell $\Omega_\bullet^\circ$ (i.e. the second projection $pr_2 : X_\bullet \to Fl(n)$ is a fibration by Schubert cells). Schubert cells are usually indexed by permutations; the bijection between checker configurations and permutations was given in Section 2.1. For example, the permutation corresponding to Figure 9 is 1324.

3.3. *The degeneration sequence.* Given a point p of $Fl(n)$ (parametrizing $F_.^{\text{moving}}$) in the dense open Schubert cell (with respect to a fixed reference flag $F_.^{\text{fixed}}$), the degeneration sequence (Section 2.1) can be interpreted as a sequence in $Fl(n)$, consisting of a chain of $\binom{n}{2}$ $\mathbb{P}^1$'s, starting at p and ending with the "most degenerate" point of $Fl(n)$ (corresponding to the reference flag $F_.^{\text{fixed}}$).

We first describe the chain informally. Each $\mathbb{P}^1$ corresponds to a move of black checkers. All but one point of the $\mathbb{P}^1$ lies in one open stratum $X_\bullet$; the remaining point (where the $\mathbb{P}^1$ meets the next component of the one-parameter degeneration) lies on an open stratum $X_{\bullet_{\text{next}}}$ of dimension one lower. If the move corresponds to the descending checker in row r dropping one row (and another checker to the left rising one row), then all components of the flags $F_.^{\text{fixed}}$ and $F_.^{\text{moving}}$ except F_r^{moving} are held fixed. For example, the geometry corresponding to the degeneration sequence for $n = 4$ is shown in Figure 2.

More precisely, there is a $\mathbb{P}^1$-fibration $X_\bullet \cup X_{\bullet_{\text{next}}} \to X_{\bullet_{\text{next}}}$; the $\mathbb{P}^1$ corresponding to a point of $X_\bullet$ described in the previous paragraph is a fiber. A useful alternate description of $X_\bullet \cup X_{\bullet_{\text{next}}}$ is given in Section 4.5.

3.4. The position of a k-plane relative to two given flags, in terms of white checkers; two-flag Schubert varieties $Y_{\circ\bullet}$ and $X_{\circ\bullet}$. Suppose two flags $F_.^{\text{moving}}$ and $F_.^{\text{fixed}}$ are in relative position given by black checker configuration $\bullet$. The position of a k-plane V relative to the two flags, up to the action of the subgroup of $GL(n)$ fixing the two flags, is determined by the table of numbers $\dim V \cap F_i^{\text{moving}} \cap F_j^{\text{fixed}}$.

This data is equivalent to the data of k white checkers on the checkerboard that are happy (see Section 2.2), with no two in the same row or column. The bijection is given as follows: the entry in the table $\dim V \cap F_i^{\text{moving}} \cap F_j^{\text{fixed}}$ is the number of white checkers in squares dominated by (i, j). See Figure 6 for example; the line $\mathbb{P}V$ is depicted as a dashed line.

If $F_.^{\text{moving}}$ and $F_.^{\text{fixed}}$ are two flags whose relative position is given by $\bullet$, let the *open two-flag Schubert variety* $Y_{\circ\bullet} \subset G(k, n)$ be the set of k-planes whose position relative to the flags is given by $\circ\bullet$; define the *closed two-flag Schubert variety* $\overline{Y}_{\circ\bullet}$ to be $\mathrm{Cl}_{G(k,n)} Y_{\circ\bullet}$. Let $X_{\circ\bullet}$ (resp. $\overline{X}_{\circ\bullet}$) in $G(k, n) \times X_\bullet$ be the *universal open (resp. closed) two-flag Schubert variety.* [19]

Note that (i) $X_{\circ\bullet} \to X_\bullet$ is an $Y_{\circ\bullet}$-fibration; (ii) $\overline{X}_{\circ\bullet} \to X_\bullet$ is an $\overline{Y}_{\circ\bullet}$-fibration, and proper; (iii) $G(k, n)$ is the disjoint union of the $Y_{\circ\bullet}$ (for fixed $\bullet$ and $F_.^{\text{fixed}}$, $F_.^{\text{moving}}$); (iv) $G(k, n) \times$

[19] open two-flag Schubert variety $Y_{\circ\bullet}$, closed two-flag Schubert variety $\overline{Y}_{\circ\bullet}$, universal two-flag Schubert variety, $X_{\circ\bullet}$, $\overline{X}_{\circ\bullet}$

$Fl(n) \times Fl(n)$ is the disjoint union of the $X_{\circ\bullet}$. *Caution:* the disjoint unions of (iii) and (iv) are not in general stratifications; Section 3.12 (a) provides a counterexample.

3.5. *Lemma. — The variety $Y_{\circ\bullet}$ is irreducible and smooth; its dimension is the sum over all white checkers w of the number of black checkers w dominates minus the number of white checkers w dominates (including itself).*

The proof is straightforward and hence omitted.

3.6. *Proposition (Initial position of white checkers). — Suppose $A = \{a_1, \ldots, a_k\}$ and $B = \{b_1, \ldots, b_k\}$ are two subsets of $\{1, \ldots, n\}$ of size k, and $F_\cdot^{moving}$ and $F_\cdot^{fixed}$ are two transverse (opposite) flags (i.e. with relative position given by $\bullet_{\text{init}}$). Then $\Omega_A(F_\cdot^{moving}) \cap \Omega_B(F_\cdot^{fixed})$ is the closed two-flag Schubert variety $\overline{Y}_{\circ_{A,B}\bullet_{\text{init}}}$.*

In the literature, these intersections are known as *Richardson varieties* [R]; see [KL] for more discussion and references.

Sketch of proof. By the Kleiman-Bertini theorem [K], $\Omega_A(F_\cdot^{\text{moving}}) \cap \Omega_B(F_\cdot^{\text{fixed}})$ is irreducible. Its general point lies in $Y_{\circ_1\bullet_{\text{init}}}$ for some configuration $\circ_1$ of white checkers, where the first coordinates of the white checkers of $\circ_1$ are given by the set A and the second coordinates are given by the set B. A short calculation using Lemma 3.5 yields $\dim Y_{\circ_1\bullet_{\text{init}}} \leq \dim Y_{\circ_{A,B}\bullet_{\text{init}}}$, with equality holding if and only if $\circ_1 = \circ_{A,B}$. (Reason: the sum over all white checkers w in $\circ_1$ of the number of black checkers w dominates is $\sum_{a\in A} a + \sum_{b\in B} b - kn$, which is independent of $\circ_1$, so $\dim Y_{\circ_1\bullet_{\text{init}}}$ is maximized when there is no white checker dominating another, which is the definition of $\circ_{A,B}$.) Then it can be checked directly that $\dim Y_{\circ_{A,B}\bullet_{\text{init}}} = \dim \Omega_A \cap \Omega_B$. As $Y_{\circ_{A,B}\bullet_{\text{init}}}$ is irreducible, the result follows. $\square$

3.7. The Geometric Littlewood-Richardson rule: deforming cycles in the Grassmannian. We can now give a geometric interpretation of Theorem 2.4 (the first version of the Geometric Littlewood-Richardson rule). We wish to compute the class (in $H_*(G(k,n))$) of the intersection of two Schubert cycles. By the Kleiman-Bertini theorem [K], this is the class of the intersection of two Schubert cells with respect to two general (transverse) flags, which by Proposition 3.6 is $[\overline{Y}_{\circ_{A,B}\bullet_{\text{init}}}]$. By a sequence of codimension 1 degenerations (corresponding to the degeneration sequence), we degenerate the two flags until they are equal. Each degeneration corresponds to a $\mathbb{P}^1$ in $G(k,n)$, where $\mathbb{A}^1 \subset X_\bullet$ and $\{\infty\} \in X_{\bullet_{\text{next}}}$. We have a $\overline{Y}_{\circ\bullet}$-fibration above $\mathbb{A}^1$. The fiber above ∞ of the closure of this fibration (in $G(k,n) \times \mathbb{P}^1$) turns out to be $\overline{Y}_{\circ_{\text{stay}}\bullet_{\text{next}}}$, $\overline{Y}_{\circ_{\text{swap}}\bullet_{\text{next}}}$ or $\overline{Y}_{\circ_{\text{stay}}\bullet_{\text{next}}} \cup \overline{Y}_{\circ_{\text{swap}}\bullet_{\text{next}}}$ (Theorem 3.9; $\circ_{\text{stay}}$ and $\circ_{\text{swap}}$ were defined in Section 2.2); the components appear with multiplicity 1. In other words, the two-flag Schubert variety degenerates to another two-flag Schubert variety, or to the union of two. Figure 6 illustrates the geometry behind the computation of $s_{(1)}^2 = s_{(1,1)} + s_{(2)}$ in $G(2,4)$.

3.8. More precisely, assume the black checker configuration $\bullet$ is in the degeneration sequence, and the white checkers are *mid-sort* (in the sense of Lemma 2.6). Consider the diagram:

$$\begin{array}{ccccc} \overline{X}_{\circ\bullet} := \mathrm{Cl}_{G(k,n)\times X_\bullet} X_{\circ\bullet} & \hookrightarrow & \mathrm{Cl}_{G(k,n)\times(X_\bullet \cup X_{\bullet_{\text{next}}})} X_{\circ\bullet} & \hookleftarrow & D_X \\ \downarrow & & \downarrow & & \downarrow \\ X_\bullet & \hookrightarrow & X_\bullet \cup X_{\bullet_{\text{next}}} & \hookleftarrow & X_{\bullet_{\text{next}}}. \end{array} \tag{1}$$

The Cartier divisor D_X is defined by fibered product.[20] Note that the vertical morphisms are proper, the vertical morphism on the left is a $\overline{Y}_{\circ\bullet}$-fibration, the horizontal inclusions on the left are open immersions, and the horizontal inclusions on the right are closed immersions.

The geometric constructions described in Section 3.7 are obtained from (1) by base changing via $\mathbb{P}^1 \to X_\bullet \cup X_{\bullet_{\text{next}}}$ (described in Section 3.3), to obtain:

$$\begin{array}{ccccc} \mathcal{Y}_{\circ\bullet} & \hookrightarrow & \mathrm{Cl}_{G(k,n)\times\mathbb{P}^1} \mathcal{Y}_{\circ\bullet} & \hookleftarrow & D_{\mathcal{Y}} \\ \downarrow & & \downarrow & & \downarrow \\ \mathbb{A}^1 & \hookrightarrow & \mathbb{P}^1 & \hookleftarrow & \{\infty\}. \end{array} \tag{2}$$

Here $\mathcal{Y}_{\circ\bullet}$, $\mathrm{Cl}_{G(k,n)\times\mathbb{P}^1} \mathcal{Y}_{\circ\bullet}$, and $D_{\mathcal{Y}}$ are defined by fibered product (or restriction) from (1). Again, the vertical morphisms are proper, the vertical morphism on the left is a $\overline{Y}_{\circ\bullet}$-fibration, the horizontal inclusions on the left are open immersions, and the horizontal inclusions on the right are closed immersions.

The informal statement of Section 3.7 can now be made precise:

3.9. *Theorem (Geometric Littlewood-Richardson rule, second version). —* $D_{\mathcal{Y}} = \overline{Y}_{\circ_{stay}\bullet_{next}}$, $\overline{Y}_{\circ_{swap}\bullet_{next}}$, *or* $\overline{Y}_{\circ_{stay}\bullet_{next}} \cup \overline{Y}_{\circ_{swap}\bullet_{next}}$.

By base change from (1) to (2), Theorem 3.9 is a consequence of the following, which is proved in Section 5. (The notation $\mathcal{Y}_{\circ\bullet}$ and $D_{\mathcal{Y}}$ will not be used hereafter.)

3.10. *Theorem (Geometric Littlewood-Richardson rule, third version). —* $D_X = \overline{X}_{\circ_{stay}\bullet_{next}}$, $\overline{X}_{\circ_{swap}\bullet_{next}}$, *or* $\overline{X}_{\circ_{stay}\bullet_{next}} \cup \overline{X}_{\circ_{swap}\bullet_{next}}$.

In other words, a particular divisor D_X (corresponding to $X_{\bullet_{\text{next}}} \subset X_\bullet \cup X_{\bullet_{\text{next}}}$) on a universal two-flag Schubert variety is another such variety, or the union of two such varieties.

3.11. Enumerative problems and checker tournaments. Suppose $\Omega_{\alpha_1}, \ldots, \Omega_{\alpha_\ell}$ are Schubert classes on $G(k,n)$ of total codimension $\dim G(k,n)$. Then (the degree of) their intersection — the solution to an enumerative problem by the Kleiman-Bertini theorem [K] — can clearly be inductively computed using the Geometric Littlewood-Richardson rule. Hence Schubert problems can be solved by counting *checker tournaments* of $\ell - 1$ games, where the input to the first game is α_1 and α_2, and for $i > 1$ the input to the i^{th} game

[20] D_X

is α_i and the output of the previous game.[21] (The outcome of each checker tournament will always be the same — the class of a point.)

3.12. Cautions. (a) The degenerations used in the Geometric Littlewood-Richardson rule follow the degeneration sequence. An arbitrary path through the Bruhat order will not work in general. For example, if $\circ\bullet$ is as shown on the left of Figure 10, then $X_{\circ\bullet}$ corresponds to points p_1 and p_2 in $\mathbb{P}^3$, lines ℓ_1 and ℓ_2 through p_1 such that ℓ_1, ℓ_2, and p_2 span $\mathbb{P}^3$, and a point $q \in \ell_1 - p_1$. Then for example $F_2^{\text{moving}} = \operatorname{span}(\ell_2, p_2)$ and the line corresponding to the point of $G(2,4)$ is $\operatorname{span}(q, p_2)$. The degeneration shown in Figure 10 (to $\bullet'$, say) corresponds to letting p_2 tend to p_1, and remembering the line ℓ_3 of approach. Then the divisor on $\mathrm{Cl}_{Fl(n)} X_{\circ\bullet}$ corresponding to $X_{\bullet'}$ parametrizes lines through p_1 contained in $\operatorname{span}(\ell_1, \ell_3)$; this is not of the form $X_{\circ'\bullet'}$ for any $\circ'$.

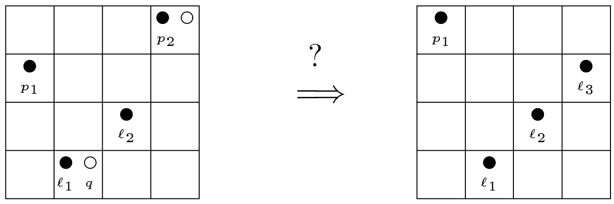

FIGURE 10. The dangers of straying from the degeneration sequence

(b) Unlike the variety $\overline{X}_\bullet = \mathrm{Cl}_{Fl(n)} X_\bullet$, the variety $\overline{X}_{\circ\bullet}$ cannot be defined numerically, i.e. in general $\overline{X}_{\circ\bullet}$ need not be

$$X'_{\circ\bullet} := \{(V, F_.^{\text{fixed}}, F_.^{\text{moving}}) \in G(k,n) \times Fl(n) \times Fl(n) : \dim V \cap F_i^{\text{fixed}} \cap F_j^{\text{moving}} \geq \gamma_\circ^{i,j}\}$$

where $\gamma_\circ^{i,j}$ is the number of white checkers dominated by (i,j). For example, in Figure 6, if $\circ\bullet$ is the configuration marked "*" and $\circ'\bullet$ is the configuration marked "**", then $X'_{\circ\bullet} = \overline{X}_{\circ\bullet} \cup \overline{X}_{\circ'\bullet}$.

4. QUILT VARIETIES

We will associate a variety to the following data.

- n is a positive integer.
- $\mathcal{P}$ is a subset of the plane (visualized so that downwards corresponds to increasing the first coordinate and rightwards corresponds to increasing the second coordinate, in keeping with the labeling convention for tables), with the partial order $\prec$ given by domination (defined in Section 3.1), and $\dim : \mathcal{P} \to \mathbb{Z}^{\geq 0}$ is a morphism of posets (i.e. order-preserving map), denoted *dimension*.[22]
- If $[\mathbf{a}, \mathbf{b}]$ is a minimal interval of $\mathcal{P}$ (i.e. $\mathbf{a}, \mathbf{b} \in \mathcal{P}$, $\mathbf{a} \prec \mathbf{b}$, and there is no $\mathbf{c} \in \mathcal{P}$ such that $\mathbf{a} \prec \mathbf{c} \prec \mathbf{b}$), then $\dim \mathbf{a} = \dim \mathbf{b} - 1$.

[21] checker tournaments
[22] dimension

- $\mathcal{P}$ has a maximum element and a minimum element.

We call this data a *planar poset*, and denote it by $\mathcal{P}$; the remaining data $(\prec, \dim, n)$ will be implicit.[23]

It will be convenient to represent this data as a planar graph, whose vertices are elements of $\mathcal{P}$, and whose edges correspond to minimal intervals of $\mathcal{P}$. The interior of the graph is a union of quadrilaterals; call these the *quadrilaterals of* $\mathcal{P}$. An element of $\mathcal{P}$ at (i,j) is said to be on the *southwest border* (resp. *northeast border*) if there are no elements of $\mathcal{P}$ (i',j') such that $i' \geq i$ and $j' \leq j$ (resp. $i' \leq i$ and $j' \geq j$); see Figure 11.[24]

Define the *quilt variety* $Q(\mathcal{P})$ to be the variety parametrizing a $(\dim \mathbf{s})$-plane $V_{\mathbf{s}}$ in K^n for each $\mathbf{s} \in \mathcal{P}$, with $V_{\mathbf{s}} \subset V_{\mathbf{t}}$ for $\mathbf{s} \prec \mathbf{t}$. (It is a closed subvariety of $\prod_{\mathbf{s}\in\mathcal{P}} G(\dim \mathbf{s}, n)$.)[25] Elements $\mathbf{s}$ of $\mathcal{P}$ will be written in bold-faced font; corresponding vector spaces will be denoted $V_{\mathbf{s}}$.

4.1. *Lemma. — The quilt variety $Q(\mathcal{P})$ is smooth.*

Proof. Consider the planar graph representation of $\mathcal{P}$ described above. The variety parametrizing the subspaces corresponding to the southwest border of the graph is a partial flag variety (and hence smooth). The quilt variety $Q(\mathcal{P})$ can be expressed as a tower of $\mathbb{P}^1$-bundles over the partial flag variety by inductively adding the data of elements of $\mathbf{s} \in S$ corresponding to "new" vertices of quadrilaterals (where the other three vertices $\mathbf{s_1} \prec \mathbf{s_2} \prec \mathbf{s_3}$ are already parametrized, and $\mathbf{s_1} \prec \mathbf{s} \prec \mathbf{s_3}$). $\square$

For example, Figure 11 illustrates that one particular quilt variety is a tower of five $\mathbb{P}^1$-bundles over $Fl(4)$; the correspondence of the $\mathbb{P}^1$-bundles with quadrilaterals is illustrated by the arrows.

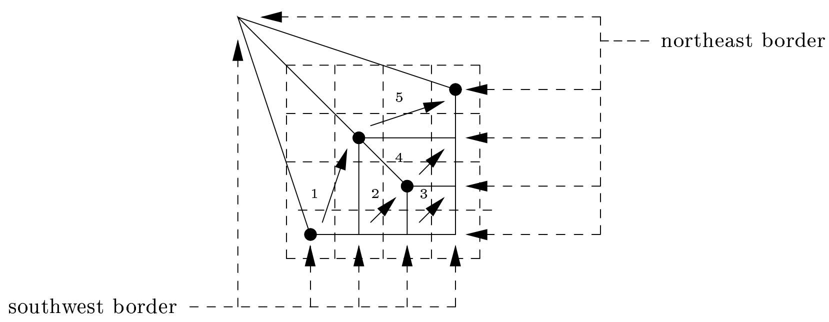

FIGURE 11. The northeast and southwest borders of a planar poset generated by a checker configuration; description of a quilt variety as a tower of five $\mathbb{P}^1$-bundles over $Fl(4)$

[23] planar poset, $\mathcal{P}$

[24] quadrilateral; southwest and northeast border

[25] quilt variety, $Q(\mathcal{P})$

4.2. *Strata of quilt varieties.* Any subset Q of the quadrilaterals of a planar poset determines a *stratum*[26] of the quilt variety. The closed stratum corresponds to requiring the subspaces of the opposite corners of the quadrilaterals in Q of the same dimension to be the same. The open stratum corresponds to also requiring the spaces of the opposite corners of the quadrilaterals *not* in Q to be distinct. By the construction in the proof of Lemma 4.1, (i) the open strata give a stratification, (ii) the closed strata are smooth, and (iii) the codimension of the stratum is the size of the subset Q. It will be convenient to depict a stratum by placing an "=" in the quadrilaterals of Q, indicating the pairs of subspaces that are required to be equal (see for example Figure 12).

4.3. *Example: planar posets generated by a set of checkers.* Given a checker configuration $\bullet$ (or $\circ$) and a positive integer n, we define the planar poset $\mathcal{P}_\bullet$ (or $\mathcal{P}_\circ$) as follows.[27] Include the squares of the table where there is a checker above (or possibly in the same square), and a checker to the left (or in the same square); include also a "zero element" above and to the left of the checkers. (The definition of happy in Section 2.2 can be rephrased as: the white checkers lie on elements of $\mathcal{P}_\bullet$.) For $\mathsf{s} \in \mathcal{P}$, let $\dim \mathsf{s}$ be the number of checkers dominated by s.

For example, if $\bullet$ is a configuration of n checkers (as in Section 2.1), then the southwest border of $\mathcal{P}_\bullet$ corresponds to F^{fixed}, and the northeast border corresponds to F^{moving}; $Q(\mathcal{P}_\bullet)$ is a fibration over $Fl(n)$ (where $Fl(n)$ parametrizes $F_.^{\text{fixed}}$), and the fiber is a Bott-Samelson resolution of $\Omega_.(F_.^{\text{fixed}})$. Figure 11 describes a Bott-Samelson resolution of the Schubert cell corresponding to 1324. Similarly, the morphism $Q(\mathcal{P}_\bullet) \to \overline{X}_\bullet$ is a resolution of singularities. This morphism restricts to an isomorphism of the dense open stratum of $Q(\mathcal{P}_\bullet)$ with $X_\bullet$. If $\bullet$ is in the degeneration sequence, then $\overline{X}_{\bullet_{\text{next}}}$ is (isomorphic to) a codimension 1 stratum of this quilt variety. See Figure 12 for an example.

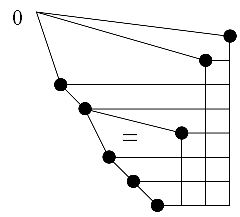

FIGURE 12. The poset corresponding to $\bullet$ of Figure 3, with the divisorial stratum corresponding to $\bullet_{\text{next}}$ marked with an "="

4.4. Quilt varieties of morphisms of posets. Suppose $\mathcal{P}$ and $\mathcal{Q}$ are two planar posets (for the same n), and $p : \mathcal{P} \to \mathcal{Q}$ is a morphism of posets (i.e. an order-preserving map of sets, with no conditions on the planar structures). Then let $Q(p) = Q(\mathcal{P} \to \mathcal{Q})$ [28] be the subvariety of $Q(\mathcal{P}) \times Q(\mathcal{Q})$ such that if $p(\mathsf{s}) = \mathsf{t}$, then the subspace corresponding to

[26] strata of a quilt variety
[27] $\mathcal{P}_\bullet, \mathcal{P}_\circ$
[28] $Q(p) = Q(\mathcal{P} \to \mathcal{Q})$

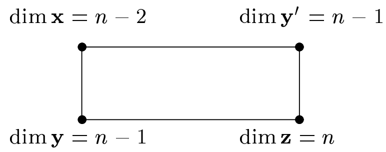

FIGURE 13. The planar poset $\mathcal{P}_\square$

s is contained in the subspace corresponding to t. For example, a configuration of black and white checkers $\circ\bullet$ induces a morphism of posets $p_{\circ\bullet} : \mathcal{P}_\circ \to \mathcal{P}_\bullet$[29], and $X_{\circ\bullet}$ is an open subset of $Q(p_{\circ\bullet} : \mathcal{P}_\circ \to \mathcal{P}_\bullet)$.

Caution: Unlike $Q(\mathcal{P})$, the quilt variety $Q(\mathcal{P} \to \mathcal{Q})$ may be singular. For example, if $\mathcal{P} = \{(x,y) : x, y \in \{0,1\}\}$, $\mathcal{Q} = \{(x,y) : x, y-1 \in \{0,1\}\}$, $p(x,y) = (x, y+1)$, and $\dim(x,y) = x+y$, then $Q(p)$ (with $n=3$) is the triangle variety (parametrizing points p_1, p_2, p_3 and lines ℓ_{12}, ℓ_{23}, ℓ_{31} in $\mathbb{P}^2$ with $p_i, p_j \in \ell_{ij}$) and hence singular. Also, $X_{\circ\bullet}$ need not be dense in $Q(\mathcal{P}_\circ \to \mathcal{P}_\bullet)$; see Section 3.12 (b).

4.5. Relating $X_\bullet \cup X_{\bullet_{\text{next}}}$ to the simpler variety $Q(\mathcal{P}_\square)$ via $X_{\bullet\square}$. Let $\mathcal{P}_\square$ be the poset of Figure 13. Then $Q(\mathcal{P}_\square)$ parametrizes hyperplanes $V_\mathbf{y}$ and $V_{\mathbf{y}'}$, and a codimension 2 subspace $V_\mathbf{x} \subset V_\mathbf{y}, V_{\mathbf{y}'}$. (Of course $V_\mathbf{z} = K^n$.) The variety $Q(\mathcal{P}_\square)$ has one divisorial stratum $D_\square$, corresponding to $V_\mathbf{y} = V_{\mathbf{y}'}$.[30] This variety will play a central role in the proof.

It will be useful to describe $X_\bullet \cup X_{\bullet_{\text{next}}}$ in terms of $Q(\mathcal{P}_\square)$ and $D_\square$. We do this by way of a variety $X_{\bullet\square}$ which is a certain open subset of $Q(p_{\bullet\square} : \mathcal{P}_\bullet \to \mathcal{P}_\square)$ (defined in Section 4.6) whose image in $Q(\mathcal{P}_\bullet)$ is $X_\bullet \cup X_{\bullet_{\text{next}}}$, where $p_{\bullet\square}$ is the morphism of posets depicted in Figure 14.[31]

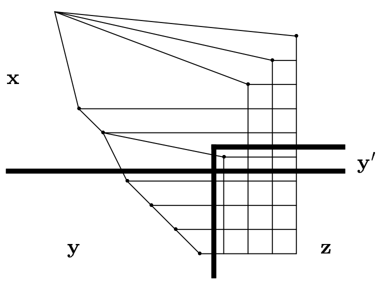

FIGURE 14. A pictorial depiction of $p_{\bullet\square} : \mathcal{P}_\bullet \to \mathcal{P}_\square$; elements of $p_{\bullet\square}^{-1}(\mathbf{x})$, $p_{\bullet\square}^{-1}(\mathbf{y})$, $p_{\bullet\square}^{-1}(\mathbf{y}')$, $p_{\bullet\square}^{-1}(\mathbf{z})$ lie in regions labeled $\mathbf{x}$, $\mathbf{y}$, $\mathbf{y}'$, $\mathbf{z}$ respectively.

[29] $p_{\circ\bullet}$

[30] $\mathcal{P}_\square, \mathbf{x}, \mathbf{y}, \mathbf{y}', \mathbf{z}, V_\mathbf{x}, V_\mathbf{y}, V_{\mathbf{y}'}, V_\mathbf{z}, D_\square$

[31] $p_{\bullet\square}$

4.6. *First description of $X_{\bullet\square}$.* Suppose the descending checker is at (r, c).[32] Let

$$S_{c-1} \subset S_c \subset \cdots \subset S_n \tag{3}$$

be the subspaces corresponding to elements of $\mathcal{P}_\bullet$ in the bottom row of the table. (Subscripts denote dimension.) Let

$$T_0 \subset T_1 \subset \cdots \subset T_n \tag{4}$$

be the subspaces corresponding to the northeast border of $\mathcal{P}_\bullet$.[33] Define $X_{\bullet\square}$[34] to be the locally closed subvariety of $(X_\bullet \cup X_{\bullet_{\text{next}}}) \times Q(\mathcal{P}_\square)$ such that

$$V_{\mathbf{x}} \cap T_{r+1} = T_{r-1}, \quad V_{\mathbf{y}'} \cap T_{r+1} = T_r, \quad V_{\mathbf{y}} \cap S_c = S_{c-1}. \tag{5}$$

Then the vector spaces corresponding to elements of $\mathcal{P}_\bullet$ are determined by $V_{\mathbf{x}}$, $V_{\mathbf{y}}$, $V_{\mathbf{y}'}$, and

$$S_c \subset S_{c+1} \subset \cdots \subset S_n, \quad T_0 \subset T_1 \subset \cdots \subset T_{r-2} \subset T_{r+1} \subset \cdots \subset T_{n-1} \subset T_n \tag{6}$$

as shown in Figure 15. (This is because each element of $\mathcal{P}_\bullet$ and $\mathcal{P}_{\bullet_{\text{next}}}$ is of the form $\inf(\mathbf{b}, \mathbf{b}')$, for some $\mathbf{b}'$ on the northeast border, and $\mathbf{b}$ in the bottom row of the table; and $V_{\inf(\mathbf{b},\mathbf{b}')} = V_{\mathbf{b}} \cap V_{\mathbf{b}'}$ for any point of $X_\bullet$ and $X_{\bullet_{\text{next}}}$. Hence $V_{\inf(\mathbf{b},\mathbf{b}')}$ is determined by (3) and (4), and thus (6) and $V_{\mathbf{x}}$, $V_{\mathbf{y}}$, $V_{\mathbf{y}'}$.)

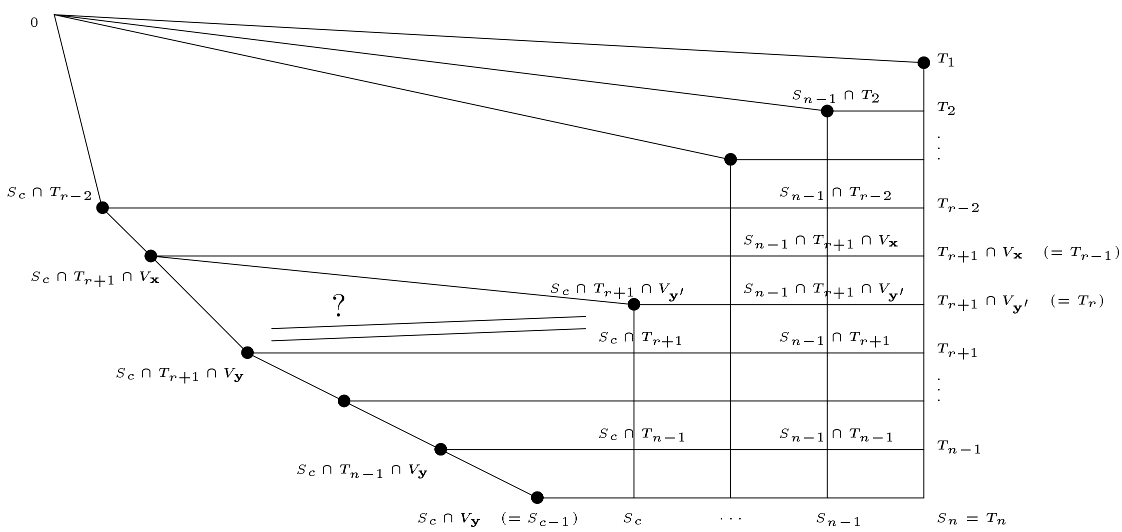

FIGURE 15. Pictorial description of the morphism $X_{\bullet\square} \to X_\bullet \cup X_{\bullet_{\text{next}}}$ (in the guise of the morphism $X_{\bullet\square} \to Q(\mathcal{P}_\bullet)$)

4.7. *Second description of $X_{\bullet\square}$.* Equivalently, $X_{\bullet\square}$ parametrizes $V_{\mathbf{x}}$, $V_{\mathbf{y}}$, $V_{\mathbf{y}'}$, and the partial flags $S_\cdot$ and $T_\cdot$ of (6) (*not* (3) and (4)), such that

- the partial flags $S_\cdot$ and $T_\cdot$ are transverse,
- $T_{r-2} \subset T_{r+1} \cap V_{\mathbf{x}}$,

[32] first use of (r, c)
[33] $S_\cdot$, $T_\cdot$
[34] $X_{\bullet\square}$

- $V_{\mathbf{x}} \subset V_{\mathbf{y}}, V_{\mathbf{y}'}$, and
- $V_{\mathbf{x}}$ is transverse to $S_c \cap T_{r+1}$. (As $r + c \geq n+1$, $\dim S_c \cap T_{r+1} \geq 2$, so $V_{\mathbf{y}}$ and $V_{\mathbf{y}'}$ are also transverse to $S_c \cap T_{r+1}$.)

If these conditions hold, we say that $V_{\mathbf{x}}$, $V_{\mathbf{y}}$, $V_{\mathbf{y}'}$, $S_\cdot$, $T_\cdot$, are in *$X_{\bullet\square}$-position*.[35]

The projection $f_{\bullet\bullet_{\text{next}}} : X_{\bullet\square} \to X_\bullet \cup X_{\bullet_{\text{next}}}$ is smooth and surjective: given an element of $X_\bullet \cup X_{\bullet_{\text{next}}}$, where $S_\cdot$ and $T_\cdot$ are the partial flags of (3) and (4), the fiber corresponds to a choice of $(V_{\mathbf{x}}, V_{\mathbf{y}}, V_{\mathbf{y}'})$ satisfying (5). More precisely, (i) let $V_{\mathbf{y}} = T_{r-1} + S_{c-1}$, (ii) then choose $V_{\mathbf{x}}$ in $V_{\mathbf{y}}$ such that $V_{\mathbf{x}} \cap T_{r+1} = T_{r-1}$ (or equivalently such that $V_{\mathbf{x}} \supset T_{r-1}$), (iii) then let $V_{\mathbf{y}'} = V_{\mathbf{x}} + T_r$.

Similarly, the morphism $f_\square : X_{\bullet\square} \to Q(\mathcal{P}_\square)$ is smooth and surjective; by the definition of $X_{\bullet\square}$-position, $f_\square$ expresses $X_{\bullet\square}$ as an open subset of a tower of projective bundles over $Q(\mathcal{P}_\square)$.

4.8. Note that $f^{-1}_{\bullet\bullet_{\text{next}}} X_{\bullet_{\text{next}}} = f_\square^{-1} D_\square$ (see Figure 15 — $V_{\mathbf{y}} = V_{\mathbf{y}'}$ iff $S_c \cap T_{r+1} \cap V_{\mathbf{y}} = S_c \cap T_{r+1} \cap V_{\mathbf{y}'}$). This will allow us to translate questions about codimension one degenerations in the degeneration sequence (involving $X_{\bullet_{\text{next}}} \subset X_\bullet \cup X_{\bullet_{\text{next}}}$) to simpler facts about codimension one degenerations relating to $D_\square \subset Q(\mathcal{P}_\square)$. The notation $f_{\bullet\bullet_{\text{next}}}$ and $f_\square$ will not be used hereafter.

5. Proof of the Geometric Littlewood-Richardson rule

We now prove (the third version of) the Geometric Littlewood-Richardson rule, Theorem 3.10.

5.1. Strategy of proof. The strategy is as follows. Instead of considering the "divisor at ∞" of the closure of $X_{\circ\bullet}$ in $G(k,n) \times (X_\bullet \cup X_{\bullet_{\text{next}}})$, we consider the corresponding divisor on closures of other sets in different sets in different spaces, shown in (7). (The varieties $X_{\circ\bullet\square}$ and $X_{\circ\square}$ will be defined in Section 5.3, and the smoothness and surjectivity of the morphisms of the top row will be established. For convenience, let Z be $\mathrm{Cl}_{Q(\mathcal{P}_\circ)\times Q(\mathcal{P}_\square)} X_{\circ\square}$.) There is a "divisor at ∞" on each of these varieties that behaves well with respect to pullback by these morphisms; it corresponds to $X_{\bullet_{\text{next}}} \subset X_\bullet \cup X_{\bullet_{\text{next}}}$ on the left and $D_\square \subset Q(\mathcal{P}_\square)$ on the right.

(7)

$$\begin{array}{ccccc}
\mathrm{Cl}_{Q(\mathcal{P}_\circ)\times\left(X_\bullet \cup X_{\bullet_{\text{next}}}\right)} X_{\circ\bullet} & \stackrel{\text{sm. surj.}}{\longleftarrow} & \mathrm{Cl}_{Q(\mathcal{P}_\circ)\times\left(X_\bullet \cup X_{\bullet_{\text{next}}}\right)} X_{\circ\bullet\square} & \stackrel{\text{sm. surj.}}{\longrightarrow} & Z := \mathrm{Cl}_{Q(\mathcal{P}_\circ)\times Q(\mathcal{P}_\square)} X_{\circ\square} \\
\downarrow \text{proper birat'l} & & & & \downarrow \text{closed imm.} \\
\mathrm{Cl}_{G(k,n)\times\left(X_\bullet \cup X_{\bullet_{\text{next}}}\right)} X_{\circ\bullet} & & & & Q(\mathcal{P}_\circ \to \mathcal{P}_\square)
\end{array}$$

We first identify the components of $\mathrm{Cl}_{Q(\mathcal{P}_\circ)\times\left(X_\bullet \cup X_{\bullet_{\text{next}}}\right)} X_{\circ\bullet}$ as follows. The components of "the divisor at ∞" of $Q(\mathcal{P}_\circ \to \mathcal{P}_\square)$ of dimension at least $\dim X_{\circ\square} - 1$ are identified by Theorem 5.7. They are denoted D^Z_S, where S is a certain set of "good quadrilaterals"

[35] $X_{\bullet\square}$-position

in the poset $\mathcal{P}_\circ$. This gives a list containing the components of the "divisor at ∞" of $Z = \mathrm{Cl}_{Q(\mathcal{P}_\circ)\times Q(\mathcal{P}_\square)} X_{\circ\square}$. Via the smooth surjective morphisms of the top row of (7), this immediately gives a list containing the components, denoted D_S, of the "divisor at ∞" of $\mathrm{Cl}_{Q(\mathcal{P}_\circ)\times\left(X_\bullet \cup X_{\bullet_{\text{next}}}\right)} X_{\circ\bullet}$.

We say D_S is *geometrically irrelevant*[36] if its image in $G(k,n)\times X_{\bullet_{\text{next}}}$ is of smaller dimension (and *geometrically relevant* otherwise). In Section 5.10, it is shown that all but one or two D_S (corresponding to those described in the Geometric Littlewood-Richardson rule) are geometrically irrelevant. We do this by exhibiting a one-parameter family through a general point of D_S contracted by the morphism to $G(k,n)\times X_{\bullet_{\text{next}}}$.

Next, in Section 5.13, we show that in the one or two geometrically relevant cases D_S appears with multiplicity one in the "divisor at ∞", by showing that D_S^Z appears with multiplicity one in the corresponding divisor on Z.

Finally, these one or two D_S's map are birational to (and hence map with degree 1 to) $X_{\circ_{\text{stay}}\bullet_{\text{next}}}$ or $X_{\circ_{\text{swap}}\bullet_{\text{next}}}$ (Proposition 5.15).

5.2. *Remark.* The bijection to puzzles [KV] gives a second proof; here is a very quick sketch. First show that D_X contains both $X_{\circ_{\text{stay}}\bullet_{\text{next}}}$ and/or $X_{\circ_{\text{swap}}\bullet_{\text{next}}}$ (Section 5.13). If $\circ\bullet$ arises in the course of a checker game starting with subsets α and β, then D_X can have no more components, and these one or two must appear with multiplicity one. Otherwise, choose any γ such that the non-zero effective cycle $D_X - \overline{X}_{\circ_{\text{stay}}\bullet_{\text{next}}}$, $D_X - \overline{X}_{\circ_{\text{swap}}\bullet_{\text{next}}}$, or $D_X - \overline{X}_{\circ_{\text{stay}}\bullet_{\text{next}}} - \overline{X}_{\circ_{\text{swap}}\bullet_{\text{next}}}$ has a non-zero coefficient of the basis element corresponding to γ. Then the number of puzzles with inputs α and β and output γ is strictly less than the Littlewood-Richardson coefficient $c_{\alpha\beta}^{\gamma}$, giving a contradiction.

One advantage of the proof presented in Section 5 is that in order to generalize the Geometric Littlewood-Richardson rule to other geometric situations (see for example Section 6), one needs the geometry behind it.

5.3. Reduction to $Q(\mathcal{P}_\square)$. We first reduce much of the argument to statements involving the poset $\mathcal{P}_\square$ (Figure 13) rather than the more complicated $\mathcal{P}_\bullet$ as follows.

The composition of $p_{\circ\bullet} : \mathcal{P}_\circ \to \mathcal{P}_\bullet$ and $p_{\bullet\square} : \mathcal{P}_\bullet \to \mathcal{P}_\square$ is the morphism $p_{\circ\square} : \mathcal{P}_\circ \to \mathcal{P}_\square$ depicted in Figure 16. Let $X_{\circ\square}$[37] be the open subset of $Q(p_{\circ\square} : \mathcal{P}_\circ \to \mathcal{P}_\square)$ such that if $\mathbf{b} \in \mathcal{P}_\circ$ and $\mathbf{c} \in \mathcal{P}_\square$, then $V_{\mathbf{b}} \subset V_{\mathbf{c}}$ if *and only if* $p_{\circ\square}(\mathbf{b}) \prec \mathbf{c}$. (One could call this a "precise quilt variety" of the morphism of posets, $PQ(p_{\circ\square})$. Then $X_{\circ\bullet} = PQ(p_{\circ\bullet})|_{X_\bullet}$, $X_{\bullet\square} = PQ(p_{\bullet\square})|_{X_\bullet\cup X_{\bullet_{\text{next}}}}$, and $PQ(p) \subset Q(p)$ is an open immersion for all p. However, to minimize notation, we will not use this terminology.)

Define $X_{\circ\bullet\square}$ as a "triple fibered product" as in Figure 17, i.e. as the indirect limit of the lower part of the figure. Equivalently, $X_{\circ\bullet\square}$ is the open subset of $X_{\circ\bullet}\times_{Q(\mathcal{P}_\circ)} X_{\circ\square}$ whose image in $Q(\mathcal{P}_\bullet)\times Q(\mathcal{P}_\square)$ is in $X_{\bullet\square}$. Note that $X_{\circ\bullet\square}$ is an open subset of both $X_{\circ\bullet}\times_{X_\bullet\cup X_{\bullet_{\text{next}}}}$

[36] geometrically (ir)relevant

[37] $p_{\circ\square}$, $X_{\circ\square}$

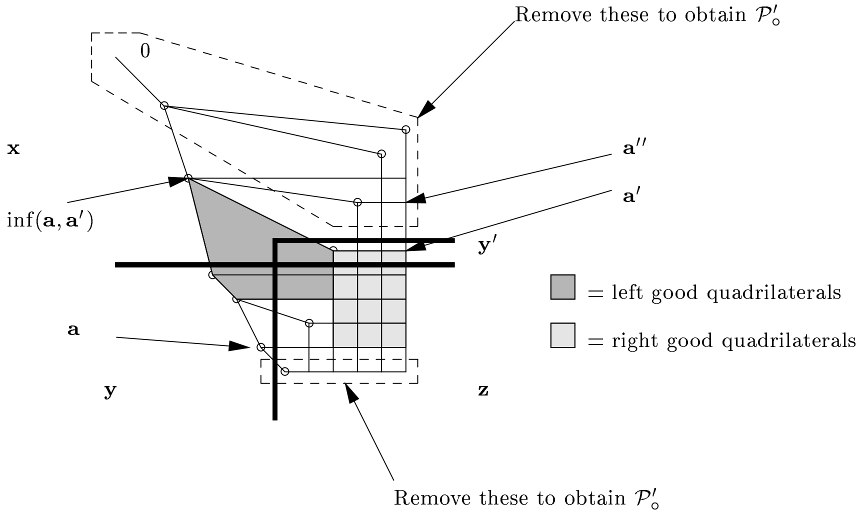

FIGURE 16. $p_{\circ\square} : \mathcal{P}_\circ \to \mathcal{P}_\square$, $\mathbf{a}$, $\mathbf{a}'$, $\mathbf{a}''$, $\mathcal{P}'_\circ$

$$\begin{tikzcd}
 & X_{\circ\bullet\square} \arrow[dl, "\text{smooth surj.}"'] \arrow[dd] \arrow[dr, "\text{smooth surj.}"] & \\
X_{\circ\bullet} \arrow[ddd] \arrow[ddr] & & X_{\circ\square} \arrow[ddl] \arrow[ddd] \\
 & X_{\bullet\square} \arrow[ddl, "\text{smooth surj.}"'] \arrow[ddr, "\text{smooth surj.}"] & \\
 & Q(\mathcal{P}_\circ) & \\
X_\bullet \cup X_{\bullet_{\text{next}}} & & Q(\mathcal{P}_\square)
\end{tikzcd}$$

FIGURE 17. The definition of $X_{\circ\bullet\square}$

$X_{\bullet\square}$ and $X_{\circ\square} \times_{Q(\mathcal{P}_\square)} X_{\bullet\square}$ (although not in general equal to either), so the projections from $X_{\circ\bullet\square}$ to $X_{\circ\bullet}$ and $X_{\circ\square}$ are both smooth (by base change from $X_{\bullet\square} \to X_\bullet \cup X_{\bullet_{\text{next}}}$ and $X_{\bullet\square} \to Q(\mathcal{P}_\square)$). In addition, $X_{\circ\bullet\square} \to X_{\circ\bullet}$ is surjective; the fiber corresponds to a certain (non-empty, open) choice of $V_{\mathbf{x}}$, $V_{\mathbf{y}}$, $V_{\mathbf{y}'}$. Similarly, $X_{\circ\bullet\square} \to X_{\circ\square}$ is surjective. This information is summarized in the top and bottom rows of (8).

$$\begin{tikzcd}
X_{\circ\bullet} \arrow[d, "\text{open}"', "\text{imm.}"] & X_{\circ\bullet\square} \arrow[l, "\text{smooth}"', "\text{surjective}"] \arrow[r, "\text{smooth}", "\text{surjective}"'] \arrow[d, "\text{open}"', "\text{imm.}"] & X_{\circ\square} \arrow[d, "\text{open}"', "\text{imm.}"] \\
\mathrm{Cl}_{Q(\mathcal{P}_\circ)\times(X_\bullet \cup X_{\bullet_{\text{next}}})} X_{\circ\bullet} \arrow[d, "\text{proper}"'] & \mathrm{Cl}_{Q(\mathcal{P}_\circ)\times X_{\bullet\square}} X_{\circ\bullet\square} \arrow[l, "\text{smooth}"', "\text{surjective}"] \arrow[r, "\text{smooth}", "\text{surjective}"'] \arrow[d, "\text{proper}"'] & Z = \mathrm{Cl}_{Q(\mathcal{P}_\circ)\times Q(\mathcal{P}_\square)} X_{\circ\square} \arrow[d, "\text{proper}"'] \\
X_\bullet \cup X_{\bullet_{\text{next}}} & X_{\bullet\square} \arrow[l, "\text{smooth}"', "\text{surjective}"] \arrow[r, "\text{smooth}", "\text{surjective}"'] & Q(\mathcal{P}_\square)
\end{tikzcd} \tag{8}$$

As remarked earlier, $\mathrm{Cl}_{Q(\mathcal{P}_\circ)\times Q(\mathcal{P}_\square)} X_{\circ\square}$ is denoted by Z.[38] The morphism

$$\mathrm{Cl}_{Q(\mathcal{P}_\circ)\times X_{\bullet\square}} X_{\circ\bullet\square} \to \mathrm{Cl}_{Q(\mathcal{P}_\circ)\times\left(X_\bullet \cup X_{\bullet_{\text{next}}}\right)} X_{\circ\bullet}$$

is smooth and surjective for the same reason that $X_{\circ\bullet\square} \to X_{\circ\bullet}$ and $X_{\bullet\square} \to X_\bullet \cup X_{\bullet_{\text{next}}}$ were: the fiber corresponds to choosing $V_{\mathbf{x}}$, $V_{\mathbf{y}}$, $V_{\mathbf{y}'}$, satisfying the requirements of $X_{\bullet\square}$-position, except the transversality conditions with the spaces corresponding to elements of $\mathcal{P}_\bullet$, so this morphism is a tower of projective bundles.

5.4. The morphism $\mathrm{Cl}_{Q(\mathcal{P}_\circ)\times X_{\bullet\square}} X_{\circ\bullet\square} \to Z$ is smooth for the same reason that $X_{\circ\bullet\square} \to X_{\circ\square}$ and $X_{\bullet\square} \to Q(\mathcal{P}_\square)$ were. More precisely, this morphism is constructed by choosing the $S_\cdot$'s and $T_\cdot$'s in (6):

(i) inductively choosing S_i (starting with $i = n$ and decrementing) so that S_i contains (the subspace corresponding to) the maximum element of $\mathcal{P}_\circ$ in column up to i, then
(ii) inductively choosing T_i (starting with $i = n$ and decrementing) so that T_i contains (the subspace corresponding to) the maximum element of $\mathcal{P}_\circ$ in row up to i, then
(iii) discarding the closed subset not in $X_{\bullet\square}$-position, and defining T_{r-1}, T_r, S_{c-1} by (5).

Note that (i) involves only the southwest border of $\mathcal{P}_\circ$ (and not the element $\mathbf{a}$ shown in Figure 16), and (ii) involves only the northeast border (and not the elements $\mathbf{a}'$ and $\mathbf{a}''$ shown in Figure 16).

5.5. Proof of the Geometric Littlewood-Richardson rule in the cases where $p_{\circ\square}^{-1}(\mathbf{y})$ or $p_{\circ\square}^{-1}(\mathbf{y}')$ is empty. This corresponds to the cases where there are no white checkers in the critical diagonal or the critical row, respectively (five of the nine cases of Table 1).

In the case $p_{\circ\square}^{-1}(\mathbf{y}') = \{\}$, the family $Z \to Q(\mathcal{P}_\square)$ is pulled back from a family over $Q(\mathcal{P}_\square - \{\mathbf{y}'\})$, the partial flag parametrizing $V_{\mathbf{x}} \subset V_{\mathbf{y}} \subset K^n$. In particular, the pullback of $D_\square = \{V_{\mathbf{y}} = V_{\mathbf{y}'}\}$ to Z consists of one component, appearing with multiplicity 1. The corresponding divisor on $\mathrm{Cl}_{Q(\mathcal{P}_\circ)\times\left(X_\bullet \cup X_{\bullet_{\text{next}}}\right)} X_{\circ\bullet}$ also appears with multiplicity 1 by the top row of (7) or the middle row of (8), and it is isomorphic to its image $\overline{X}_{\circ_{\text{stay}}\bullet_{\text{next}}}$ in $\overline{X}_{\circ\bullet}$.

The same argument holds for the case $p_{\circ\square}^{-1}(\mathbf{y}) = \{\}$, with the roles of $\mathbf{y}$ and $\mathbf{y}'$ switched.

5.6. Proof in the remaining cases. For the rest of Section 5, we assume that both $p_{\circ\square}^{-1}(\mathbf{y})$ (the critical diagonal) and $p_{\circ\square}^{-1}(\mathbf{y}')$ (the critical row) are non-empty. The white checkers are in mid-sort, by Lemma 2.6. Let $\mathbf{a}$ (resp. $\mathbf{a}'$, $\mathbf{a}''$) be the maximum[39] of $p_{\circ\square}^{-1}(\mathbf{y})$ (resp. $p_{\circ\square}^{-1}(\mathbf{y}')$, $p_{\circ\square}^{-1}(\mathbf{x})$), so $V_{\mathbf{a}}$, $V_{\mathbf{a}'}$, $V_{\mathbf{a}''}$ are the corresponding subspaces. (See Figure 16.)

In lieu of studying the components of the preimage of $D_\square$ on Z, we find the components of the pullback of $D_\square$ to the (a priori larger) variety $Q(\mathcal{P}_\circ \to \mathcal{P}_\square)$, and show that they all have dimension at most $\dim X_{\circ\square} - 1$.

[38] Z
[39] $\mathbf{a}$,$\mathbf{a}'$, $\mathbf{a}''$

The pullback of $D_\Box$ to $Q(\mathcal{P}_\circ \to \mathcal{P}_\Box)$ is best described in terms of the stratification of $Q(\mathcal{P}_\circ)$. Define the *good quadrilaterals* of $\mathcal{P}_\circ$ to be those quadrilaterals whose minimal element does not dominate a, and either (a) whose minimal element dominates the white checker $\min(p_{\circ\Box}^{-1}(\mathbf{y}'))$ in the critical row $p_{\circ\Box}^{-1}(\mathbf{y}')$, or (b) with two vertices dominating $\min(p_{\circ\Box}^{-1}(\mathbf{y}'))$, and two vertices in $p_{\circ\Box}^{-1}(\{\mathbf{x}, \mathbf{y}\})$. Call those in case (a) *right good quadrilaterals* and those in case (b) *left good quadrilaterals*; see Figure 16. Note that the good quadrilaterals appear in columns,[40] and that, if there is a blocker, there is no column to the left of the white checker in the critical row $\min(p_{\circ\Box}^{-1}(\mathbf{y}'))$ (i.e. no left good quadrilaterals).

The following theorem describes the pullback of $D_\Box$ to $Q(\mathcal{P}_\circ \to \mathcal{P}_\Box)$.

5.7. *Theorem. — The components of the pullback of $D_\Box$ to $Q(\mathcal{P}_\circ \to \mathcal{P}_\Box)$ of dimension at least $\dim X_{\circ\Box} - 1$ correspond to sets of good quadrilaterals, with at most one quadrilateral in each column, as follows. If S is such a set of good quadrilaterals, the corresponding component is the closure of the pullback to $Q(\mathcal{P}_\circ \to \mathcal{P}_\Box)$ of the open stratum on $Q(\mathcal{P}_\circ)$ corresponding to S. Its dimension is exactly $\dim X_{\circ\Box} - 1$.*

Let D_S^Z be the component corresponding to S. Let D_S be the corresponding subvariety of $Q(\mathcal{P}_\circ) \times X_{\bullet_{\text{next}}}$ (obtained via the top row of (7) or the middle row of (8)).[41]

Proof. We note first that $X_{\circ\Box}$ can be constructed by starting with the dense open stratum of $Q(\mathcal{P}_\circ)$, then choosing $V_\mathbf{y}$ containing $V_\mathbf{a}$ and $V_{\mathbf{a}''}$ (giving a dimensional contribution of $n - (\dim \mathbf{a} + \dim \mathbf{a}'' - \dim \inf(\mathbf{a}, \mathbf{a}'))$, as $V_\mathbf{a} \cap V_{\mathbf{a}''} = V_{\inf(\mathbf{a},\mathbf{a}')}$ for an element of the dense open stratum), then choosing $V_{\mathbf{y}'}$ containing $V_{\mathbf{a}'}$ (giving a dimensional contribution of $n - \dim \mathbf{a}'$). Then $V_\mathbf{x} = V_\mathbf{y} \cap V_{\mathbf{y}'}$ is determined. Hence

$$\dim X_{\circ\Box} = 2n - \dim \mathbf{a} - \dim \mathbf{a}' - \dim \mathbf{a}'' + \dim \inf(\mathbf{a}, \mathbf{a}'). \tag{9}$$

Next, consider an irreducible component of the pullback of $D_\Box$ to $Q(\mathcal{P}_\circ \to \mathcal{P}_\Box)$ of dimension at least $\dim X_{\circ\Box} - 1$. We will show that its dimension is precisely this, and that the component is of the form described in Theorem 5.7.

Let $\ell = \dim(V_\mathbf{a} \cap V_{\mathbf{a}'}) - \dim \inf(\mathbf{a}, \mathbf{a}')$ for a general point of this component. (Note that $\ell \geq 0$, as $V_\mathbf{a} \cap V_{\mathbf{a}'}$ contains $V_{\inf(\mathbf{a},\mathbf{a}')}$.) Let $Q_\ell \subset Q(\mathcal{P}_\circ)$ be the locus where $\dim(V \cap V') = \ell + \dim \inf(\mathbf{a}, \mathbf{a}')$.[42] Then a dense open subset U of the component with a morphism to Q_ℓ, and U is an open set of the fibration over Q_ℓ parametrizing choices of $V_\mathbf{y} = V_{\mathbf{y}'}$ containing $V_\mathbf{a}$ and $V_{\mathbf{a}'}$ (giving a dimensional contribution of $n - (\dim V_\mathbf{a} + \dim V_{\mathbf{a}'} - \dim(V_\mathbf{a} \cap V_{\mathbf{a}'}))$), and $V_\mathbf{x}$ contained in $V_\mathbf{y} = V_{\mathbf{y}'}$ containing $V_{\mathbf{a}''}$ (giving a dimensional contribution of $n - 1 - \dim V_{\mathbf{a}''}$ once $V_\mathbf{y} = V_{\mathbf{y}'}$ is chosen). Thus by Proposition 5.8 below,

$$\begin{aligned}
\dim U &\leq \dim Q_\ell + (n - \dim \mathbf{a} - \dim \mathbf{a}' + (\ell + \dim \inf(\mathbf{a}, \mathbf{a}'))) + (n - 1 - \dim \mathbf{a}'') \\
&= (\dim Q_\ell + \ell) + 2n - \dim \mathbf{a} - \dim \mathbf{a}' - \dim \mathbf{a}'' + \dim \inf(\mathbf{a}, \mathbf{a}') - 1 \\
&\leq \dim X_{\circ\Box} - 1 \qquad \text{(by (9))},
\end{aligned}$$

[40] left and right good quadrilaterals, columns
[41] D_S^Z, D_S
[42] Q_ℓ

and if equality holds, then the the component is of the form desired (also by Proposition 5.8). ☐

5.8. *Proposition.* — *The irreducible components of Q_ℓ have codimension at least ℓ in $Q(\mathcal{P}_\circ)$, and those components of codimension exactly ℓ are strata of the form described in Theorem 5.7.*

Proof. Suppose $\mathcal{P}'_\circ$[43] is defined by removing from $\mathcal{P}_\circ$ all rows below $\mathbf{a}$, and all elements of $p_{\circ\square}^{-1}(\mathbf{x})$ except $\inf(\mathbf{a}, \mathbf{a}')$ (see Figure 16). As in the proof of Lemma 4.1, the natural morphism $Q(\mathcal{P}_\circ) \to Q(\mathcal{P}'_\circ)$ is a tower of projective bundles , and the components of Q_ℓ on $Q(\mathcal{P}_\circ)$ are precisely the pullback of components of the analogous Q_ℓ on $Q(\mathcal{P}'_\circ)$. Hence the Proposition follows from the analogous result for $Q(\mathcal{P}'_\circ)$, Proposition 5.9. ☐

More precisely, it suffices to prove the result for $\mathcal{P}'_\circ$ of the following form. Fix $r_1 < \cdots < r_y$ and $c_1 < \cdots < c_x$ where $x, y > 1$, and $r_1 < R_1 < \cdots < R_z < r_y$ and $c_2 > C_1 > \cdots > C_z > c_1$ ((R_i, C_i) will be location of white checkers not contained in the grid $\{(r_i, c_j)\}$, for example a blocker). Then $\mathcal{P}'_\circ$ is the poset generated by the set $\{(r_1, c_i)\}_{1 \leq i \leq x} \cup \{(r_i, c_1)\}_{1 \leq i \leq y} \cup \{(R_i, C_i)\}_{1 \leq i \leq z}$ (see Section 4.3, and Figure 18 for an example). Note that the critical row corresponds to $\{(r_1, c_2), \ldots, (r_1, c_x)\}$, the critical diagonal corresponds to $\{(r_2, c_1), \ldots, (r_y, c_1)\}$, $\mathbf{a} = (r_y, c_1)$, $\mathbf{a}' = (r_1, c_x)$, and $\inf(\mathbf{a}, \mathbf{a}') = (r_1, c_1)$.

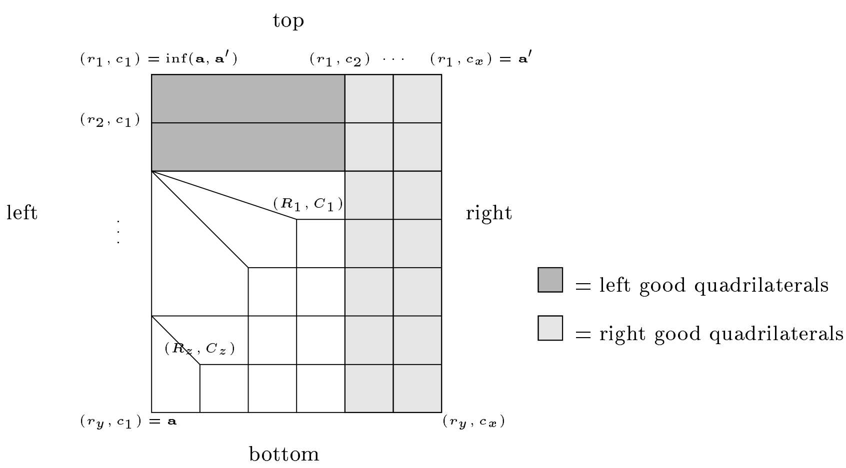

FIGURE 18. An example of $\mathcal{P}'_\circ$

5.9. *Proposition.* — *The irreducible components of Q_ℓ on $Q(\mathcal{P}'_\circ)$ (described in the previous paragraph) have codimension at least ℓ in $Q(\mathcal{P}'_\circ)$, and those components of codimension exactly ℓ are strata of the form described in Theorem 5.7 (corresponding to sets of good quadrilaterals, at most one per column).*

Proof. For convenience, we assume $\dim \inf(\mathbf{a}, \mathbf{a}') = 0$. (Geometrically, this corresponds to considering instead the quotient of all subspaces by $V_{\inf(\mathbf{a},\mathbf{a}')}$.)

[43] $\mathcal{P}'_\circ$

Fix an irreducible component of Q_ℓ of codimension at most ℓ, and choose a general point of this component; this corresponds to some configuration of subspaces $\{V_{\mathbf{c}} \subset K^m : \mathbf{c} \in \mathcal{P}'_\circ\}$. Label each element $\mathbf{c}$ of $\mathcal{P}'_\circ$ with $\dim(V_{\mathbf{c}} \cap V_{\mathbf{a}})$. Hence the label on any vertex dominating $\mathbf{a}$ is $\dim \mathbf{a}$, and the label on $\mathbf{a}'$ is ℓ. The label on any $\mathbf{c} \in \mathcal{P}'_\circ$ is at most $\dim \mathbf{c}$.

This point lies in some open stratum of $Q(\mathcal{P}'_\circ)$; mark the quadrilaterals corresponding to that stratum with "=". Then each labeled quadrilateral looks like one of the examples in Figure 19.

We argue by induction on the number of good quadrilaterals. The base case is given in *(c)* and *(d)* below, and the inductive step is given in *(a)* and *(b)*.

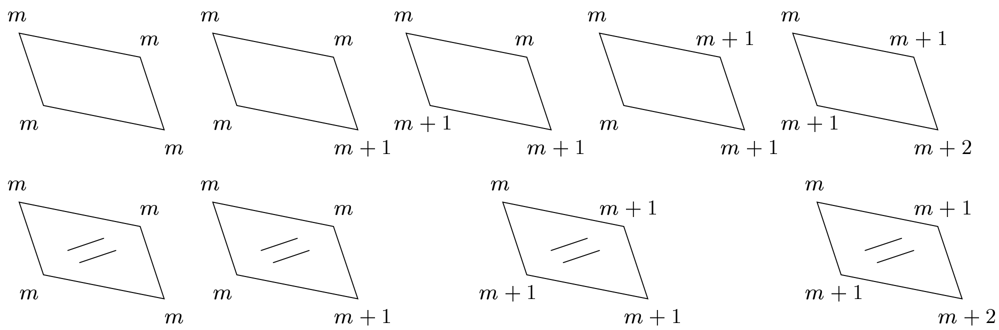

FIGURE 19. Possible quadrilaterals in proof of Proposition 5.9 (where $\mathbf{c}$ is labeled with $\dim(V_{\mathbf{c}} \cap V_{\mathbf{a}})$)

(a) First, if $x > 2$, consider the right-most column of good quadrilaterals (see Figure 20). The two vertices in the bottom row are labeled $\dim \mathbf{a}$, and the vertex in the upper right is labeled ℓ. The vertex in the upper left of the column is labeled either $\ell - 1$ or ℓ. If it is labeled ℓ, then the resulting poset with the right-most column of vertices removed also satisfies the hypothesis of the Proposition, and hence by the inductive hypothesis there must be at least ℓ equal signs further to the left, of the desired form (all good quadrilaterals, at most one per column). Hence the Proposition holds in this case.

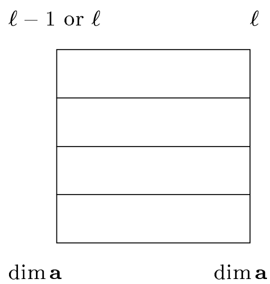

FIGURE 20. The right-most column of quadrilaterals (in case (a) of the proof of Proposition 5.9)

If otherwise the vertex in the upper left corner of the right-most column of quadrilaterals is labeled $\ell-1$, then by the inductive hypothesis there must be at least $\ell-1$ equal signs further to the left, of the desired form. Furthermore, by inspection of Figure 19, there must be another equal sign in the right-most column as well, and again the Proposition holds. See Figure 21 for an example.

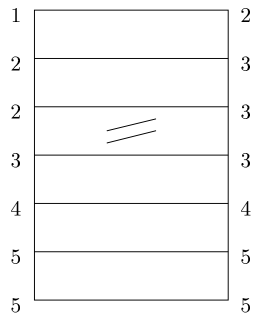

FIGURE 21. Sample labeling of the right-most column of quadrilaterals (in case (a) of the proof of Proposition 5.9)

(b) Next suppose $x = 2$ (so there are no right good quadrilaterals), and there is at least one left good quadrilateral (hence there is no blocker). Let $\mathbf{w} = (r_1, c_2)$ (the rightmost element of the top row; this corresponds to the white checker in the critical row of $\circ$). The label on $\mathbf{w}$ must be 0 or 1, as $\dim \mathbf{w} = 1$. If $\mathbf{w}$ has label 0, then the Proposition follows immediately. If $\mathbf{w}$ has label 1, then the top left quadrilateral must be of one of the forms shown in Figure 22. In each case, we can remove the top two vertices of the good quadrilateral, and in all but the first case subtract 1 from each of the other vertices (as shown in Figure 22), and reduce to the case with one fewer good quadrilaterals. Hence by the inductive hypothesis, the last case cannot happen (there must be a second "=" in a good quadrilateral further below, yet we are allowed only $\ell = 1$). The other cases may occur, and by our inductive hypothesis the Proposition holds.

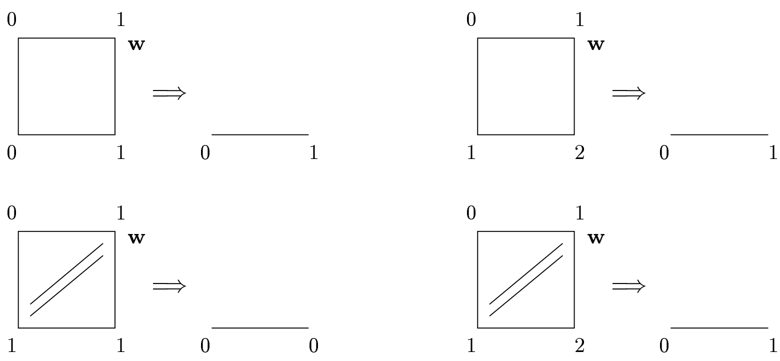

FIGURE 22. The top (left) good quadrilateral (in case (b) of the proof of Proposition 5.9)

(c) Next, if there are no good quadrilaterals, and no blockers, then the labeled poset is the one shown in Figure 23, and the result is immediate.

FIGURE 23. The trivial case (i)(c) of the proof of Proposition 5.9

(d) Finally, suppose there are no good quadrilaterals (implying $x = 2$), and there is a blocker. As in *(b)*, $\ell = 0$ or 1. If $\ell = 0$, the Proposition is immediate.

Assume now that $\ell = 1$; we will obtain a contradiction. Re-label the poset by labeling element $\mathbf{c}$ with the dimension of the intersection of its corresponding vector space with $V_{\mathbf{a}'}$ (rather than $V_{\mathbf{a}}$). Hence all labels are 0 or 1, and the elements on the right side and the bottom of the graph are labeled 1. Any quadrilateral with minimal element labeled 0 and other three elements labeled 1 must be marked with an "=" (see Figure 24). By hypothesis, as the component of Q_1 has codimension at most 1 in $Q(\mathcal{P}'_\circ)$, there can be at most one such quadrilateral. As the subset of elements labeled 0 has a maximum, which doesn't lie on the right side or the bottom of the graph, there is at least one such quadrilateral, so there is exactly one. The component of Q_1 lies in the (irreducible) divisorial stratum corresponding to this quadrilateral, so these two loci are equal. Thus a general point of this divisorial stratum lies in Q_1.

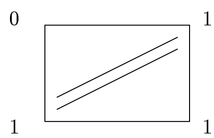

FIGURE 24.

We construct the divisorial stratum as a tower of $\mathbb{P}^1$-bundles over the partial flag variety parametrizing the subspaces corresponding to the vertices on the northeast border (as in the proof of Lemma 4.1, where the southwest border was used). There can be no quadrilateral labeled as in Figure 25 (with no "="): $V_{\mathbf{e}}$ is a general subspace (of $\dim \mathbf{e}$) containing $V_{\mathbf{c}}$ and contained in $V_{\mathbf{f}}$; as $\dim V_{\mathbf{d}} \cap V_{\mathbf{a}'} = 0$, we have $\dim V_{\mathbf{e}} \cap V_{\mathbf{a}'} = 0$ as well, so the label on the lower left vertex must be 0, not 1.

Now consider the part of the graph above row r_2, as in Figure 26. As there are no quadrilaterals marked as in Figure 25, all unlabeled vertices in Figure 26 must have label 1 (work inductively bottom to top, and left to right in each row), contradicting the fact that there is precisely one quadrilateral marked as in Figure 24. $\square$

5.10. Geometric irrelevance of all but one or two divisors. We next show that all but one or two of the $D_S \subset Q(\mathcal{P}_\circ) \times X_{\bullet_{\text{next}}}$ (defined immediately after the statement of

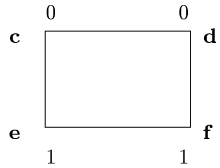

FIGURE 25.

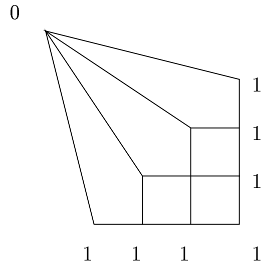

FIGURE 26.

Theorem 5.7) are geometrically irrelevant. Note that $D_{\{\}}$ corresponds to the entry "stay" in Table 1, and $D_{\{\text{top left good quad.}\}}$ corresponds to "swap".

Proposition 5.11 shows that all other components are geometrically irrelevant, and Proposition 5.12 shows that $D_{\{\}}$ is geometrically irrelevant as well when required to be by Table 1.

The following example may motivate the argument. Suppose $\circ\bullet$ is the configuration of black and white checkers shown in Figure 27, corresponding to planes in $\mathbb{P}^3$. Then a general point of $X_{\circ\bullet}$ is depicted in Figure 28. The four points parametrized by black checkers are denoted b_1, b_2, b_3, b_4, and the three points parametrized by the white checkers are denoted p_1, p_2, p_3. The other subspaces parametrized by $Q(\mathcal{P}_\circ)$ are two lines l_{12} and l_{23} (containing $\{p_1, p_2\}$ and $\{p_2, p_3\}$ respectively), and a plane f_{123}. For a fixed point of $X_\bullet$, this locus clearly has dimension 2, (generically) one for the choice of p_2 on the line b_2b_3 and one for the choice of p_3 on the line b_3b_4.

In the degeneration corresponding to $X_{\bullet_{\text{next}}}$, b_2 tends to b_1 (and the line of approach ℓ is remembered). Note that there are two good quadrilaterals in $\mathcal{P}'_\circ$, one "left" and one "right"; denote them L and R. There are then three possible degenerations of Figure 28 (i.e. three components of D'_X), depicted in Figure 29.

The first corresponds to the subset $S = \{L\}$, and is geometrically *relevant*. For a fixed point of $X_{\bullet_{\text{next}}}$, this locus visibly has dimension 2, one for the choice of l_{12} through $p_1 = p_2 = b_1 = b_2$ in the plane spanned by ℓ and b_3, and one for the choice of p_3 on the line b_3b_4.

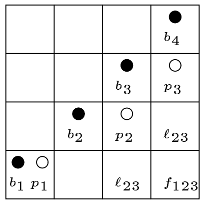

FIGURE 27.

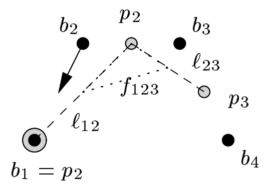

FIGURE 28. A general point of $X_{\circ\bullet}$ (where $\circ\bullet$ is given in Figure 27)

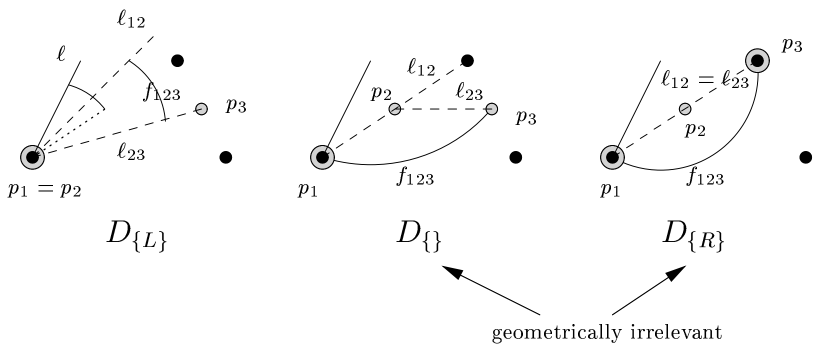

FIGURE 29. Degenerations of Figure 28 (planes are denoted by arcs; a plane contains a line if the arc meets the line)

The second corresponds to the subset $S = \{\}$, and is geometrically *irrelevant*. For a fixed point of $X_{\bullet_{\text{next}}}$, this locus visibly has dimension 2, one for the choice of p_2 on the line b_1b_3, and one for the choice of p_3 on the line b_3b_4. However, the image in $G(3,4) = \mathbb{G}(2,3)$ has dimension 1, as the plane f_{123} depends only on the choice of p_3. This observation is a special case of Proposition 5.12.

The third corresponds to the subset $\{R\}$, and is also geometrically *irrelevant*. For a fixed point of $X_{\bullet_{\text{next}}}$, this locus visibly has dimension 2, one for the choice of p_2 on the line b_1b_3, and one for the choice of the plane f_{123} containing the line b_1b_3. Again, the image in $G(3,4)$ has dimension 1. This observation is a special case of Proposition 5.11.

Note that there is no component corresponding to $S = \{L, R\}$, as as the locus $Q_{\ell=2}$ on $Q(\mathcal{P}_\circ)$ is empty (as $\dim \mathbf{a} = \dim \mathbf{a}' = 1$, so $\ell := \dim V_{\mathbf{a}} \cap V_{\mathbf{a}'} - \dim V_{\inf(\mathbf{a},\mathbf{a}')} \leq 1 - 0 = 1$).

5.11. *Proposition. — If $S \neq \{\}, \{$top left good quad.$\}$, then D_S is geometrically irrelevant.*

Proof. Note that the projection

$$\mathrm{Cl}_{Q(\mathcal{P}_\circ)\times(X_\bullet \cup X_{\bullet_{\text{next}}})} X_{\circ\bullet} \to \mathrm{Cl}_{G(k,n)\times(X_\bullet \cup X_{\bullet_{\text{next}}})} X_{\circ\bullet}$$

involves forgetting all elements of $\mathcal{P}_\circ$ but the maximum, and that its construction (given in Section 5.4) depends only on the vector spaces on the northeast and southeast borders of $\mathcal{P}_\circ$. Fix a general point of D_S^Z (corresponding to a configuration of subspaces $\{V_{\mathbf{c}} \subset K^n : \mathbf{c} \in \mathcal{P}_\circ\}$). It will suffice to produce a one-parameter family through this point that preserves the spaces in the northeast and southwest borders. All possibilities for S fall into at least one of the following three cases.

Case 1: S contains a left good quadrilateral that is not the top left good quadrilateral. Name the elements of $\mathcal{P}_\circ$ as in Figure 30 (showing the quadrilateral in question). Then a one-parameter family corresponds to fixing all $V_{\mathbf{m}}$ ($\mathbf{m} \in \mathcal{P}_\circ$) except $V_{\mathbf{d}}$, and letting $V_{\mathbf{d}}$ move freely in $\mathbb{P}(V_{\mathbf{b}}/V_{\mathbf{e}}) \cong \mathbb{P}^1$.

(Note that this would fail if the left good quadrilateral were at the top. In this case, $p_{\circ\square}(\mathbf{d}) = \mathbf{x}$, but the $V_{\mathbf{d}}$ corresponding to a general element of $\mathbb{P}(V_{\mathbf{b}}/V_{\mathbf{e}})$ would lie in $V_{\mathbf{y}} = V_{\mathbf{y}'}$, and not necessarily in $V_{\mathbf{x}}$.)

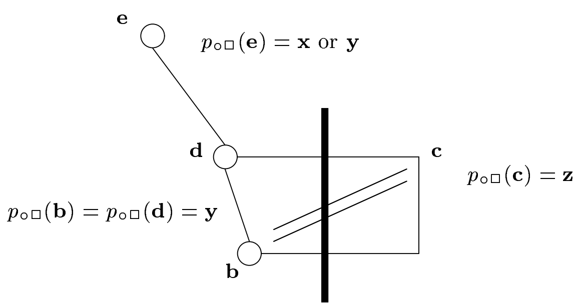

FIGURE 30. Case 1 of Proposition 5.11

Case 2: S contains a right good quadrilateral q, and no quadrilaterals in the column directly to the left of q, and at least as high as q. Name the elements of $\mathcal{P}_\circ$ as in Figure 31. The desired one-parameter family corresponds to fixing all the vector spaces $V_{\mathbf{m}}$ ($\mathbf{m} \in \mathcal{P}_\circ$) except for $V_{\mathbf{d}}, V_{\mathbf{g_1}}, \dots, V_{\mathbf{g_m}}$, and choosing $V_{\mathbf{d}}$ from an open set of $\mathbb{P}(V_{\mathbf{b}}/V_{\mathbf{e}}) \cong \mathbb{P}^1$, such that $V_{\mathbf{g_i}} := V_{\mathbf{d}} \cap V_{\mathbf{h_i}}$ has dimension $\dim \mathbf{g_i}$ ($1 \leq i \leq m$). Note that $V_{\mathbf{f_i}}$ is automatically contained in $V_{\mathbf{g_i}}$ as $V_{\mathbf{g_i}} = V_{\mathbf{d}} \cap V_{\mathbf{h_i}}$ contains $V_{\mathbf{e}} \cap V_{\mathbf{h_i}} = V_{\mathbf{f_i}}$ by construction.

Case 3: S contains a right good quadrilateral q, and another good quadrilateral in the column directly to the left of q, at least as high as q. Name the elements of $\mathcal{P}_\circ$ as in Figure 32. Then the argument from the Case 2 applies verbatim. $\square$

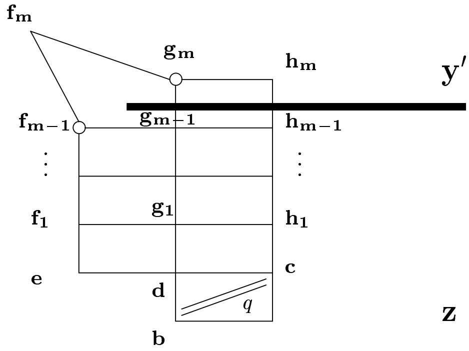

FIGURE 31. Case 2 of Proposition 5.11

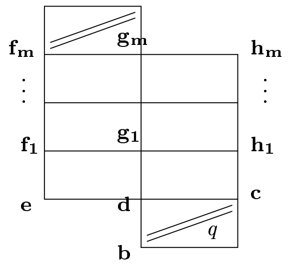

FIGURE 32. Case 3 of Proposition 5.11

5.12. *Proposition. — If $S = \{\}$ and (i) the white checker in the critical row is in the descending checker's square, or (ii) the white checker in the critical diagonal is in the rising checker's square, then D_S is geometrically irrelevant.*

Proof. We deal with case (ii); case (i) is essentially identical and hence omitted.

As in the proof of Proposition 5.11, we note that the construction of Section 5.4 depended only on the vector spaces on the northeast and southeast borders of $\mathcal{P}_\circ$, but *not* the vector space on the northeast border in the critical row. Hence it will suffice to produce a one-parameter family through a general point of D_S^Z that preserves the spaces in the northeast and southwest borders, except the element of the critical row.

Name the elements of $\mathcal{P}_\circ$ as in Figure 33. As the point of D_S^Z maps to the dense open stratum of $Q(\mathcal{P}_\circ)$, we have $V_{\mathbf{h_i}} = V_{\mathbf{c}} + V_{\mathbf{g_i}}$; as $V_{\mathbf{c}} \subset V_{\mathbf{y}} = V_{\mathbf{y'}}$ and $V_{\mathbf{g_i}} \subset V_{\mathbf{y'}}$, we have $V_{\mathbf{h_i}} \subset V_{\mathbf{y}}$ as well. The desired one-parameter family corresponds to fixing all the vector spaces $V_{\mathbf{l}}$ ($\mathbf{l} \in \mathcal{P}_\circ$) except for $V_{\mathbf{d}}$, $V_{\mathbf{g_1}}, \dots, V_{\mathbf{g_m}}$, and choosing $V_{\mathbf{d}}$ from an open set of $\mathbb{P}(V_{\mathbf{b}}/V_{\mathbf{e}}) \cong \mathbb{P}^1$, such that $V_{\mathbf{g_i}} := V_{\mathbf{d}} + V_{\mathbf{f_i}}$ has dimension $\dim \mathbf{g_i}$ $(1 \leq i \leq m)$. $\square$

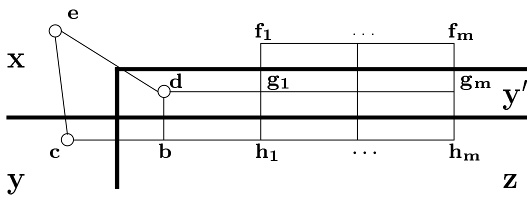

FIGURE 33.

5.13. Multiplicity 1. We have shown that at most one or two of the components of D'_X are geometrically relevant. We now show that these one or two components appear with multiplicity 1 in $\mathrm{Cl}_{Q(\mathcal{P}_\circ)\times\left(X_\bullet \cup X_{\bullet_{\mathrm{next}}}\right)} X_{\circ\bullet}$. By the top row of (7) or the middle row of (8), it suffices to prove that the analogous divisors on Z appear with multiplicity 1.

5.14. *Proposition. —*

(a) *The divisor $D^Z_{\{\}}$ is contained in the pullback of $D_\square$ with multiplicity 1.*
(b) *The divisor $D^Z_{\{\text{top left good quad.}\}}$ is contained in the pullback of $D_\square$ with multiplicity 1 if there is no blocker (i.e. there is a top left good quadrilateral).*

Proof. (a) It suffices to verify the result in the preimage of the dense open stratum of $Q(\mathcal{P}_\circ)$; it then suffices to verify the result for a fixed point of $Q(\mathcal{P}_\circ)$. Here

$$V_{\mathbf{a}} \cap V_{\mathbf{a}'} = V_{\mathbf{a}} \cap V_{\mathbf{a}''} = V_{\inf(\mathbf{a},\mathbf{a}')}.$$

The Proposition then reduces to a straightforward (hence omitted) local calculation about the locus in $Q(\mathcal{P}_\square)$ such that $V_{\mathbf{x}}$ contains $V_{\mathbf{a}''}$, $V_{\mathbf{y}}$ contains $V_{\mathbf{a}}$, and $V_{\mathbf{y}'}$ contains $V_{\mathbf{a}'}$ (where $V_{\mathbf{a}}$, $V_{\mathbf{a}'}$, $V_{\mathbf{a}''}$ are fixed).

(b) It suffices to verify the result in the preimage of the union of the dense open stratum of $Q(\mathcal{P}_\circ)$ and the (divisorial) open stratum of $Q(\mathcal{P}_\circ)$ corresponding to $\{$top left good quad.$\}$. This union admits a $\mathbb{P}^1$-fibration to the divisorial stratum of $Q(\mathcal{P}_\circ)$, and it suffices to verify the result for a fixed fiber as follows. Name the elements of $\mathcal{P}_\circ$ as in Figure 33. (Note that $\mathbf{a}' = \mathbf{g_m}$, $\mathbf{a}'' = \mathbf{f_m}$, $\mathbf{e} = \inf(\mathbf{a}, \mathbf{a}')$.) Hold fixed all the spaces of $\mathcal{P}_\circ$ except those in the critical row $\{V_{\mathbf{d}}, V_{\mathbf{g_1}}, \dots, V_{\mathbf{g_m}}\}$. The space $V_{\mathbf{d}}$ corresponding to the white checker varies in $\mathbb{P}(V_{\mathbf{b}}/V_{\mathbf{e}})$, and $V_{\mathbf{g_i}}$ is defined to be $V_{\mathbf{d}} + V_{\mathbf{f_i}}$. The Proposition then reduces to a straightforward (hence omitted) local calculation about the space parametrizing $(V_{\mathbf{x}}, V_{\mathbf{y}}, V_{\mathbf{y}'}, V_{\mathbf{d}})$ such that $V_{\mathbf{d}}$ varies in the pencil, $V_{\mathbf{x}}$ contains the fixed space $V_{\mathbf{f_m}}$, $V_{\mathbf{y}}$ contains the fixed space $V_{\mathbf{a}}$, and $V_{\mathbf{y}'}$ contains $V_{\mathbf{g_m}} = V_{\mathbf{d}} + V_{\mathbf{f_m}}$. □

Finally, we show that the map from D_S to $\mathrm{Cl}_{G(k,n)\times\left(X_\bullet \cup X_{\bullet_{\mathrm{next}}}\right)} X_{\circ\bullet}$ is birational to $\overline{X}_{\circ_{\mathrm{stay}}\bullet_{\mathrm{next}}}$ or $\overline{X}_{\circ_{\mathrm{swap}}\bullet_{\mathrm{next}}}$; this will conclude the proof of the Geometric Littlewood-Richardson rule.

5.15. *Proposition.* — *(a)* $D_{\{\}}$ *is birational to* $\overline{X}_{\circ_{stay}\bullet_{next}}$. *(a)* $D_{\{\text{top left good quad.}\}}$ *is birational to* $\overline{X}_{\circ_{swap}\bullet_{next}}$.

Proof. (a) The open subset of $D_{\{\}}$ contained in the preimage of the dense open stratum of $Q(\mathcal{P}_\circ)$ is isomorphic to $X_{\circ_{\text{stay}}\bullet_{\text{next}}}$. *Sketch of reason:* The subspaces parametrized by the dense open stratum are determined by the subspaces corresponding to the white checkers. (For $\mathbf{c} \in \mathcal{P}_\circ$, $V_\mathbf{c} = \operatorname{span}(V_\mathbf{w})$, where $\mathbf{w}$ runs over the white checkers dominated by $\mathbf{c}$.) As in the construction of Section 5.4, choose (i) S_i to contain those $V_\mathbf{w}$ where $\mathbf{w}$ is a white checker in column at most i, and to contain no $V_\mathbf{w}$ where $\mathbf{w}$ is a white checker in column greater than i, and (ii) T_i analogously. This gives a subset of the "divisor at ∞" of $\operatorname{Cl}_{Q(\mathcal{P}_\circ)\times\left(X_\bullet \cup X_{\bullet_{\text{next}}}\right)} X_{\circ\bullet\square}$ whose image in $\operatorname{Cl}_{Q(\mathcal{P}_\circ)\times\left(X_\bullet \cup X_{\bullet_{\text{next}}}\right)} X_{\circ\bullet}$ is $X_{\circ_{\text{stay}}\bullet_{\text{next}}}$.

(b) The open subset of $D_{\{\text{top left good quad.}\}}$ contained in the preimage of the divisorial open stratum of $Q(\mathcal{P}_\circ)$ corresponding to {top left good quad.} is isomorphic to $X_{\circ_{\text{swap}}\bullet_{\text{next}}}$. *Sketch of reason:* The subspaces parametrized by the divisorial open stratum are determined by the subspaces corresponding to

(i) the white checkers of $\circ$, except the white checkers at the opposite corners of the top left good quadrilateral (call them $\mathbf{w_1} = (r_1, c_1)$, $\mathbf{w_2} = (r_2, c_2)$, with $r_1 > r_2$, $c_1 < c_2$),
(ii) the vector space $V_{\mathbf{w_1}} = V_{\mathbf{w_2}}$, and
(iii) $V_{\sup(\mathbf{w_1},\mathbf{w_2})}$ (corresponding to the lower right corner of the top left good quadrilateral).

We can interpret these subspaces as follows. Identify $\mathbf{w_1}$ and $\mathbf{w_2}$ of $\mathcal{P}_\circ$ to obtain the poset $\mathcal{P}_{\circ_{\text{swap}}}$. The spaces described above correspond to those elements of $\mathcal{P}_{\circ_{\text{swap}}}$ with exactly one edge to a lower-dimensional element (i.e. those $\mathbf{w}$ such that there is a unique minimal interval $\mathbf{w}' \prec \mathbf{w}$). They also correspond to the white checkers of $\circ_{\text{swap}}$. As in (a), the image in $\operatorname{Cl}_{Q(\mathcal{P}_\circ)\times\left(X_\bullet \cup X_{\bullet_{\text{next}}}\right)} X_{\circ\bullet}$ is (naturally isomorphic to) $X_{\circ_{\text{swap}}\bullet_{\text{next}}}$. (The white checker of $\circ_{\text{swap}}$ corresponding $V_{\mathbf{w_1}} = V_{\mathbf{w_2}}$ must lie in the intersection of the spaces where $V_{\mathbf{w_1}}$ and $V_{\mathbf{w_2}}$ were required to lie, in the definition of $X_{\circ\bullet}$. Hence this checker lies in (r_2, c_1). The white checker of $\circ_{\text{swap}}\bullet_{\text{next}}$ corresponding to $V_{\sup(\mathbf{w_1},\mathbf{w_2})}$ is required to lie in (r_1, c_2), as it was in $X_{\circ\bullet}$.) ☐

6. Applications

6.1. Schubert problems are enumerative over the reals. A classical question of enumerative geometry is whether a Schubert problem can have all its solutions defined over $\mathbb{R}$. Suppose $\alpha_1, \dots, \alpha_m$ are k-subsets of $\{1, \dots, n\}$ such that

$$\dim\left(\Omega_{\alpha_1} \cup \cdots \cup \Omega_{\alpha_m}\right) = 0.$$

The Schubert problem corresponding to $\alpha_1, \dots, \alpha_m$ is said to be *enumerative over* $\mathbb{R}$ if there are m flags $F_\cdot^1, \dots, F_\cdot^m$ defined over $\mathbb{R}$ such that

$$\Omega_{\alpha_1}(F_\cdot^1) \cap \cdots \cap \Omega_{\alpha_m}(F_\cdot^m)$$

consists of

$$\deg\left(\Omega_{\alpha_1} \cup \cdots \cup \Omega_{\alpha_m}\right)$$

(distinct) real points. For a detailed history of this problem, see for example [S1].

6.2. *Corollary to the Geometric Littlewood-Richardson rule. — All Schubert problems for all Grassmannians are enumerative over $\mathbb{R}$. For a fixed m, there is a set of m flags that works for all choices of $\alpha_1, \ldots, \alpha_m$.*

The case $G(1,n)$ is trivially linear algebra. Sottile proved the result for $G(2,n)$ for all n, [S2], and for all problems involving only Pieri classes [S5]; see [S3] for further discussion. The argument here follows Sottile's philosophy. Note that the proof below carries through with $\mathbb{R}$ replaced by any field satisfying the implicit function theorem, such as $\mathbb{Q}_p$.

Proof of Corollary 6.2. Say the real subvariety $Z \subset G(k,n)$ is *ℓ-good* if there exist ℓ real flags $F_\cdot^1, \ldots, F_\cdot^\ell$ so that for *all* choices of $\alpha_1, \ldots, \alpha_\ell$ (k-subsets of $\{1,\ldots,n\}$) such that

$$\dim\left([Z] \cup \Omega_{\alpha_1} \cup \cdots \cup \Omega_{\alpha_\ell}\right) = 0,$$

$Z \cap \Omega_{\alpha_1}(F_\cdot^1) \cap \cdots \cap \Omega_{\alpha_\ell}(F_\cdot^\ell)$ consists of $\deg([Z] \cup \Omega_{\alpha_1} \cup \cdots \cup \Omega_{\alpha_\ell})$ real points.

As $G(k,n)$ is 1-good, it suffices to show that for $\ell \geq 1$, if Z is ℓ-good then Z is $(\ell+1)$-good. This is a consequence of Lemma 6.3 below: if Z is ℓ-good, and $F_\cdot^1, \ldots, F_\cdot^\ell$ are the real flags (of the definition of ℓ-goodness), then Lemma 6.3 applied to $Z \cap \Omega_{\alpha_1}(F_\cdot^1) \cap \cdots \cap \Omega_{\alpha_{\ell-1}}(F_\cdot^{\ell-1})$ for all $\alpha_1, \ldots, \alpha_{\ell-1}$ implies that Z is $(\ell+1)$-good (by taking $F_\cdot^{\ell+1}$ to be any $F_\cdot^{\text{moving}}$ in the intersection over all $(\alpha_1, \ldots, \alpha_{\ell-1})$ of the open subsets $U_{\bullet_{\text{init}}}$ of Lemma 6.3). $\square$

Let $\Omega_\bullet^\circ \subset Fl(n)$ be the open Schubert cell corresponding to $\bullet$. Let $\overline{\mathcal{X}}_{\circ\bullet} \subset Fl(n) \times G(k,n)$ be the "two-flag Schubert cell" corresponding to $\circ\bullet$, defined as the restriction of $\overline{X}_{\circ\bullet} \subset Fl(n) \times Fl(n) \times G(k,n)$ to where $F_\cdot^{\text{fixed}}$ is fixed in $Fl(n)$. Define $\mathcal{X}_{\circ\bullet}$ as the restriction of $X_{\circ\bullet}$ similarly.

6.3. *Lemma. — Suppose the real subvariety $Z \subset G(k,n)$ and the real flag $F_\cdot^{\textit{fixed}}$ are given such that for all α with $\dim([Z] \cup \Omega_\alpha) = 0$, $Z \cap \Omega_\alpha(F_\cdot^{\textit{fixed}})$ consists of $\deg([Z] \cup \Omega_\alpha)$ distinct real points. Then there is a sequence of non-empty open subsets (in the* classical *topology) $U_{\bullet_{\text{final}}} \subset \Omega_{\bullet_{\text{final}}}^\circ, \ldots, U_{\bullet_{\text{init}}} \subset \Omega_{\bullet_{\text{init}}}^\circ$ where $U_\bullet \cup U_{\bullet_{\textit{next}}}$ is an open neighborhood of $U_{\bullet_{\textit{next}}}$ in $Omega_\bullet^\circ \cup \Omega_{\bullet_{\textit{next}}}^\circ$, such that for all $[F_\cdot^{\textit{moving}}] \in U_\bullet$, and all $\circ\bullet$ with $\circ$ mid-sort and $\dim([Z] \cup [\overline{\mathcal{X}}_{\circ\bullet}]) = 0$, $Z \cap \overline{\mathcal{X}}_{\circ\bullet}$ consists of $\deg([Z] \cup [\overline{\mathcal{X}}_{\circ\bullet}])$ (distinct) real points.*

Proof. We prove the existence of $(U_{\bullet_{\text{final}}}, \ldots, U_{\bullet_{\text{next}}}, U_\bullet)$ by induction on $\bullet$. The base case $\bullet = \bullet_{\text{final}}$ is true by hypothesis. Assume now that $\bullet \neq \bullet_{\text{final}}$, and that $U_{\bullet_{\text{final}}}, \ldots, U_{\bullet_{\text{next}}}$ have been constructed

Fix $\circ$ (mid-sort). Consider

$$\begin{array}{cl} Z \cap \overline{\mathcal{X}}_{\circ\bullet} & \subset G(k,n) \times \left(\Omega^\circ_\bullet \cup \Omega^\circ_{\bullet_{\text{next}}}\right) \\ \downarrow f & \\ \Omega^\circ_\bullet \cup \Omega^\circ_{\bullet_{\text{next}}}. & \end{array}$$

For any $[F_.^{\text{moving}}] \in U_{\bullet_{\text{next}}}$, $f^{-1}([F_.^{\text{moving}}])$ consists of the correct number of distinct real points. (If both $\circ_{\text{stay}}$ and and $\circ_{\text{swap}}$ occur, by the inductive hypothesis this is true for both cases separately. The two sets of real points do not intersect, as they lie in different two-flag Schubert varieties $\mathcal{X}_{\circ_{\text{stay}}\bullet_{\text{next}}}$ and $\mathcal{X}_{\circ_{\text{swap}}\bullet_{\text{next}}}$.) Hence there is a neighborhood $U_{\circ\bullet}$ of $U_{\bullet_{\text{next}}}$ in $\Omega^\circ_\bullet \cup \Omega^\circ_{\bullet_{\text{next}}}$ such that this still holds. Here we are using the implicit function theorem: If $X \to Y$ is a finite degree d morphism of varieties over $\mathbb{R}$, and $p \in Y$ is a real point with d pre-images, necessarily real, then there is an analytic neighborhood of p in Y for which this is still the case.

Finally, let $U_\bullet = \cap_\circ U_{\circ\bullet} \cap \Omega^\circ_\bullet$. As each $U_{\circ\bullet}$ is a neighborhood of $U_{\bullet_{\text{next}}}$ in $\Omega^\circ_\bullet \cup \Omega^\circ_{\bullet_{\text{next}}}$, $U_\bullet$ is as well. This completes the induction. $\square$

6.4. Corollary to the Geometric Littlewood-Richardson rule: Effective numerical solutions (over $\mathbb{C}$) to all Schubert problems for all Grassmannians. Suppose $\alpha_1, \dots, \alpha_m$ are given, such that $\dim(\Omega_{\alpha_1} \cup \cdots \cup \Omega_{\alpha_m}) = 0$. By the Kleiman-Bertini theorem [K], if $F_.^1$, $\dots$, $F_.^m$ are general flags then $\Omega_{\alpha_1}(F_.^1) \cap \cdots \cap \Omega_{\alpha_m}(F_.^m)$ consists of $\deg(\Omega_{\alpha_1} \cup \cdots \cup \Omega_{\alpha_m})$ points.

The Geometric Littlewood-Richardson rule gives an algorithm for actually numerically finding these points, to any given accuracy. To the author's knowledge, previously there was no known universal method of numerically solving Schubert problems. (Of course, in any given case, the problem could be translated into Plucker coordinates, but this is in practice unworkable in general.) This generalizes [HSS] (which deal with the case of intersections of Pieri classes); the philosophy of explicit homotopies follows [HSS]. The method will be described in detail in [SV]; we only sketch it here.

We use the philosophy that if $f : V \to W$ is a degree d generically finite morphism with a good geometric description, such that for some $w \in W$, $f^{-1}(w)$ consists of d points that can be calculated numerically, then for any other $w' \in W$ such that $f^{-1}(w')$ has dimension 0, the points of $f^{-1}(w')$ can be calculated numerically as well.

Redefine the complex subvariety $Z \subset G(k,n)$ to be ℓ-good if there are ℓ flags $F_.^1$, $\dots$, $F_.^\ell$ such that for all choices of $\alpha_1, \dots, \alpha_\ell$ such that $\dim([Z] \cup \Omega_{\alpha_1} \cup \cdots \cup \Omega_{\alpha_\ell}) = 0$, $Z \cap \Omega_{\alpha_1}(F_.^1) \cap \cdots \cap \Omega_{\alpha_\ell}(F_.^\ell)$ consists of $\deg([Z] \cup \Omega_{\alpha_1} \cup \cdots \cup \Omega_{\alpha_\ell})$ points which can be numerically computed. Then the proof of Corollary 6.2 (verbatim) shows that $G(k,n)$ is ℓ-good for all ℓ. The only required modification is to take $U_\bullet$ in Lemma 6.3 to be the largest Zariski-open set such that for all $[F_.^{\text{moving}}] \in U_\bullet$, and all $\circ\bullet$ where $\circ$ is mid-sort and $\dim([Z] \cup [\overline{\mathcal{X}}_{\circ\bullet}]) = 0$, $Z \cap \mathcal{X}_{\circ\bullet}$ consists of $\deg([Z] \cup [\mathcal{X}_{\circ\bullet}])$ distinct points.

Hence given a Schubert problem with a finite number of solutions, once branch paths are chosen, the solutions can be numerically computed, and are in bijection with checker tournaments (Section 3.11).

6.5. Toward a Geometric Littlewood-Richardson rule for Flag manifolds. The same methods can be applied to Flag manifolds, in the hope of addressing the important open problem of finding a Littlewood-Richardson rule in this context (i.e. structure coefficients for the multiplication of Schubert polynomials). **I should give some references here.** We describe some partial results here, informally.

Define two-flag Schubert cells X_δ of Flag manifolds analogously to $X_{\circ\bullet}$, as the locus in $Fl(n) \times Fl(n) \times Fl(n)$ parametrizing (i) two flags $F_\cdot^{\text{fixed}}$ and $F_\cdot^{\text{moving}}$ in relative position given by $\bullet$, and (ii) a third flag $F_\cdot$ such that $\dim F_i^{\text{fixed}} \cap F_j^{\text{moving}} \cap F_k = \delta_{ijk}$. The configuration $\bullet$ is obtained from the rank table $(\delta_{ijn})i, j$ by the bijection of Section 3.1. The choice of the data δ_{ijk} for which this data is non-empty can be usefully summarized in two (equivalent) ways. It is not yet clear which is the more convenient notation.

First, these δ correspond to configurations of checkers on an $n \times n$ board, where there are i checkers labeled i for $1 \leq i \leq n$. No two checkers with the same label are in the same column or the same row. An i-checker ($i < n$) is *happy* if there is an $(i+1)$-checker to its left (or in the same square) and an $(i+1)$-checker above it (or in the same square). (See for example Figure 34.) The bijection to δ is given as follows: δ_{ijk} is the number of k-checkers dominated by (i, j). The morphism to $X_\bullet$ corresponds to forgetting all but the n-checkers.

Second, these δ correspond to "wiring diagrams", with n wires entering the board from below and leaving the board on the right. The bijection to δ is given as follows: δ_{ijk} is the number of wires numbered at least k dominated by (i, j). See Figure 35 for an example.

$\delta =$

				54
			5	
54				32
		5	432	1
	543			

$\stackrel{??}{\Longrightarrow}$ $\delta' =$

				54
			54	3
54			3	2
	543		2	1
		5		

FIGURE 34. Is the two-flag Schubert cell on the right in the closure of the one on the left?

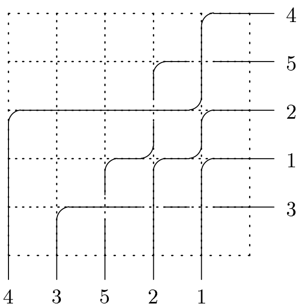

FIGURE 35. The "wiring diagram" corresponding to the first checker configuration of Figure 34

There is an analog of Proposition 3.6, describing the intersection of two Schubert cells (with respect to transverse flags $F_\cdot^{\text{fixed}}$ and $F_\cdot^{\text{moving}}$) as $\overline{X}_\delta$ for an explicitly given δ; call the set of δ obtained in such a way the *initial positions*.

6.6. *Conjecture (Existence of a Geometric Littlewood-Richardson rule for Flag manifolds). — There exists a subset M of the $\{(\delta_{ijk})_{ijk}\}$, where the configuration of n-checkers is in the degeneration sequence (analogous to "mid-sort"), containing the set of initial positions, such that the divisor D_X on $\overline{X}_\delta$ corresponding to the next element of the degeneration sequence is the union of varieties of the form $\overline{X}_{\delta'}$, each appearing with multiplicity 1, where $(\delta'_{ijk})_{ijk} \in M$.*

This conjecture (which parallels Theorem 3.10) looks quite weak, as it specifies neither (i) the "mid-sort" property M nor (ii) how to determine δ'. However, it suffices to obtain the applications described above (reality and numerical calculation of solutions to all Schubert problems). Furthermore, it implies the existence of a Littlewood-Richardson rule, and an answer to (ii) would give an explicit rule.

6.7. *Proposition. — Conjecture 6.6 is true for $n < 6$.*

This is a considerable amount of evidence, involving $\sum_{n=1}^{5} \binom{n}{2} \sum_{\alpha,\beta,\gamma} c_{\alpha\beta}^{\gamma}$ degenerations. However, there are two serious reasons to remain suspicious: (a) Knutson's puzzle variant computes Littlewood-Richardson coefficients for $n < 6$ but fails for $n = 6$ (and puzzles are related to checkers via [KV]), and (b) all Littlewood-Richardson coefficients are 0 or 1 for $n < 6$. Note that the proof of Corollary 6.2 applies without change to give the following.

6.8. *Corollary. — All Schubert problems for $Fl(n)$ are enumerative over $\mathbb{R}$ for $n < 6$. For a fixed m, there is a set of m flags that works for all choices of $\alpha_1, \dots, \alpha_m$.*

Sketch of proof of Proposition 6.7 for $n \leq 4$. We build M inductively, starting with the set of initial positions. Successively, for each element δ of M, we find a list of possible divisors $\overline{X}_{\delta'}$ on $\overline{X}_\delta$ (above $X_{\bullet_{\text{next}}}$) as follows. If the n-checkers of δ are in position $\bullet$, the n-checkers of δ' are in position $\bullet_{\text{next}}$. Then given the positions of the k-checkers of δ and the $(k+1)$-checkers of δ' (for $1 \leq k < n$), we list the (finite number of) possibilities of the choice of positions of the choices of k-checkers of δ' subject to two conditions: the k-checkers are happy, and $\delta'_{ijk} \geq \delta_{ijk}$. We then discard all δ' such that $\dim X_{\delta'} < \dim X_\delta - 1$. Then each component of D_X lies in $D_{\delta'}$ for some remaining δ'. If any $X_{\delta'}$ has dimension at least $\dim X_\delta$, we stop, and the process fails. Otherwise, D_X must consist of a union of these $X_{\delta'}$, possibility with multiplicity. We then add these δ' to M. (This is a greedy algorithm, which sometimes includes δ' which do not correspond to components of D_X.) Thus the conjecture is true for this δ (with this choice of M) with the possible exception of the multiplicity 1 claim. We now repeat the process with this enlarged M.

For $n \leq 4$, one checks (most easily by computer) that this process never fails. Moreover, as all Littlewood-Richardson coefficients for $n \leq 4$ are 1, the multiplicity must be 1 at each stage. □

The author has a full description of the degenerations which actually appear for $n \leq 4$, available upon request. However, it is not clear how to generalize this to a conjectural Littlewood-Richardson rule.

For $n = 5$, this process fails at six cases (where $\dim X_{\delta'} = \dim X_\delta$). However, in three of the six cases, it can be shown that $\overline{X}_\delta$ does not meet $X_{\delta'}$ (one is shown in Figure 34; the other two are identical except for the position of the 1-checker), and in the other three cases, δ itself can be removed from M (i.e. δ was falsely included in M by the greediness of the algorithm).

For larger n, this greedy algorithm will certainly produce even worse pathologies (i.e. arbitrarily many cases where $\dim X_{\delta'} - \dim X_\delta$ is arbitrarily large).

6.9. Other questions. We sketch here further questions and problems, some of which are work in progress.

(1) Find bijections to other Littlewood-Richardson rules. For example, currently there is no bijection known between puzzles and older rules.
(2) Apply these to other groups. For example, Leonardo Mihalcea is looking for a similar rule for the Lagrangian Grassmannian LG.
(3) Anders Buch has conjectured a checker rule for Littlewood-Richardson coefficients in K-theory. In the central entry of Table 1, there is an additional term, of one lower dimension, with a minus sign. It is a"sub-swap"; if the two white checkers in question are at (r_1, c_1) and (r_2, c_2), with $r_1 > r_2$ and $c_1 < c_2$, then they move to (r_2, c_1) and $(r_1 - 1, c_2)$. Geometrically it is "clear" to me why this rule should work — the set $X_{\circ_{\text{stay}}\bullet_{\text{next}}} \cap X_{\circ_{\text{swap}}\bullet_{\text{next}}}$ is homotopic to Anders' locus. It would be good to turn this into a proof, and I hope to talk with Anders about this at some point. Via the bijection to puzzles of [KV], Buch's conjecture turns into a conjecture of Terry Tao. More precisely, Buch's conjecture translates into the existence of a new "K-theory puzzle piece": an equilateral triangle of side 2, point downwards, with sides (clockwise from the upper left) 010101. Hence there is a triality in K-theory that is not obvious, although Anders has given me a proof.
(4) Can equivariant Littlewood-Richardson coefficients be understood geometrically in this way? For example, can the Knutson-Tao puzzles for equivariant cohomology be translated to checkers? Can this be combined with Buch's/Tao's conjecture to yield a Littlewoood-Richardson rule in equivariant K-theory? I'd like to discuss this further with Allen.
(5) The case of two-step flags is intermediate between Grassmannians and flags. It is of interest for several reasons. First, quantum cohomology of Grassmannians has been reduced to the cohomology of two-step flag varieties. Second, Allen has a conjectured rule that has been verified by Anders up to something huge, perhaps $n = 11$, so there is a conjecture in the language of puzzles that I will soon try to translate to checkers (and compare with my own thoughts on checkers, as in Section 6.5). I hope to talk with Allen about this soon.
(6) David Eisenbud asked the following question. Eisenbud and Harris have a particular (irreducible, one-parameter) path in the flag variety, whose general point is in the large open Schubert cell, and whose special point is the smallest cell: consider

the osculating flag $F_\cdot^{\text{moving}}$ to a point p on a rational normal curve, as p tends to a reference point q with osculating flag $F_\cdot^{\text{fixed}}$, [EH]. Is the degeneration sequence some sort of limit of such paths? This would provide a single path that breaks intersections of Schubert cells into their components.

REFERENCES

[B] A. S. Buch, *A Littlewood-Richardson rule for the K-theory of Grassmannians*, preprint 2000, math.AG/0004137.

[EH] D. Eisenbud and J. Harris. Their paper where they have a rational normal curve.

[EGH] Y. Eliashberg, A. Givental, H. Hofer; their SFT papers (motivation).

[Fo] S. Fomin. Bill mentioned that he had a survey of LR articles. Could he be referring to S. Fomin and C. Greene, *A Littlewood-Richardson miscellany*, Eur. J. of Comb. **14** (1993), 191–212? I will check, but it appears not from the mathscinet review.

[F] W. Fulton, *Young Tableau with Applications to Representation Theory and Geometry*, Cambridge U.P., New York, 1997.

[HSS] B. Huber, F. Sottile, and B. Sturmfels, *Numerical Schubert calculus*, J. Symbolic Comput. **26** (1998), no. 6, 767–788.

[K] S. Kleiman, *The transversality of a general translate*, Compositio Math. **28** (1974), 287–297.

[KT] A. Knutson and T. Tao, *Puzzles and (equivariant) cohomology of Grassmannians*, preprint 2001, math.AT/0112150.

[KTW] A. Knutson, T. Tao, and C. Woodward, *The honeycomb model of $GL(n)$ tensor products II: Puzzles give facets of the L-R cone*, preprint 2001, math.CO/0107011, J. Amer. Math. Soc., to appear.

[KV] A. Knutson and R. Vakil, current discussions.

[KL] V. Kreiman and V. Lakshmibai, *Richardson varieties in the Grassmannian*, preprint 2002, math.AG/0203278.

[M] D. Monk, *The geometry of flag manifolds*, Proc. London Math. Soc. **9** (1959), 253–286.

[R] R. W. Richardson, *Intersections of double cosets in algebraic groups*, Indag. Math., (N.S.), **3** (1992), 69–77.

[S1] F. Sottile, *Enumerative geometry for real varieties*, in Algebraic Geometry, Santa Cruz, 1995, J. Kollár et al ed., vol. 56, Part 2 of Proc. Sympos. Pure Math., Amer. Math. Soc., 1997.

[S2] F. Sottile, *Enumerative geometry for the real Grassmannian of lines in projective space*, Duke Math. J., **87** (1997), pp. 59–85.

[S3] F. Sottile, *Real enumerative geometry and effective algebraic equivalence*, J. Pure and App. Alg. **117** and **118** (1997), 601–615.

[S4] F. Sottile, *Pieri's formula via explicit rational equivalence*, Can. J. Math, **46** (1997), 1281–1298.

[S5] F. Sottile, *The special Schubert calculus is real*, ERA of the AMS **5** (1999), pp. 35–39.

[S6] F. Sottile, *Real rational curves in Grassmannians*, J. Amer. Math. Soc. **13** (2000), 333-341.

[S7] F. Sottile, *Some real and unreal enumerative geometry for Flag manifolds*, Michigan Math. J. **48** (2000), 573–592.

[SV] F. Sottile and R. Vakil, work in progress.

[V] R. Vakil, *The enumerative geometry of rational and elliptic curves in projective space*, J. Reine Angew. Math. (Crelle) **529** (2000), 101–153. (motivation)

DEPT. OF MATHEMATICS, STANFORD UNIVERSITY, STANFORD CA 94305–2125

E-mail address: `vakil@math.stanford.edu`